JGR Biogeosciences

RESEARCH ARTICLE
10.1029/2022JG006981

A Continental-Scale Estimate of Soil Organic Carbon Change at NEON Sites and Their Environmental and Edaphic Controls

Jie Hu[1], Alfred E. Hartemink[1], Ankur R. Desai[2], Philip A. Townsend[3], Rose Z. Abramoff[4,5], Zhe Zhu[6], Debjani Sihi[7], and Jingyi Huang[1]

[1]Department of Soil Science, University of Wisconsin-Madison, Madison, WI, USA, [2]Department of Atmospheric and Oceanic Sciences, University of Wisconsin-Madison, Madison, WI, USA, [3]Department of Forest and Wildlife Ecology, University of Wisconsin-Madison, Madison, WI, USA, [4]Climate and Ecosystem Sciences Division, Lawrence Berkeley National Laboratory, Berkeley, CA, USA, [5]Ronin Institute, Montclair, NJ, USA, [6]Department of Natural Resources and the Environment, University of Connecticut, Storrs, CT, USA, [7]Department of Environmental Sciences, Emory University, Atlanta, GA, USA

Key Points:

- The NEON sites were estimated to have large soil organic carbon (SOC) loss in both topsoil and subsoil during 1984–2014
- The carbon sequestration potential is limited in well-developed and near carbon-saturated soils in managed ecosystems
- Runoff/erosion and leaching, vertical translocation, and mineral sorption are dominant factors affecting SOC variation at National Ecological Observatory Network sites

Supporting Information:

Supporting Information may be found in the online version of this article.

Correspondence to:

J. Huang,
jhuang426@wisc.edu

Citation:

Hu, J., Hartemink, A. E., Desai, A. R., Townsend, P. A., Abramoff, R. Z., Zhu, Z., et al. (2023). A Continental-scale estimate of soil organic carbon change at NEON sites and their environmental and edaphic controls. *Journal of Geophysical Research: Biogeosciences*, *128*, e2022JG006981. https://doi.org/10.1029/2022JG006981

Received 3 MAY 2022
Accepted 25 APR 2023

Author Contributions:

Conceptualization: Alfred E. Hartemink, Jingyi Huang
Formal analysis: Jie Hu
Methodology: Jie Hu, Alfred E. Hartemink, Ankur R. Desai, Zhe Zhu, Jingyi Huang
Visualization: Jie Hu
Writing – original draft: Jie Hu, Jingyi Huang

Abstract Current carbon cycle models focus on the effects of climate and land-use change on primary productivity and microbial-mineral dependent carbon turnover in the topsoil, while less attention has been paid to vertical soil processes and soil-dependent response to land-use change along the profile. In this study, a spatial-temporal analysis was used to estimate soil organic carbon (SOC) change in topsoil/A horizon and subsoil/B horizon at National Ecological Observatory Network (NEON) sites, USA over 30 years. To separate the effects of land-use, environmental, and edaphic factors on SOC change, space-for-time substitution was used in combination with the Continuous Change Detection and Classification algorithm and Structural Equation Modeling. Results showed that (a) under natural vegetation, Spodosols and Inceptisols found in the eastern NEON sites had substantial topsoil SOC accumulation (+0.4 to +1.2 Mg C ha^{-1} $year^{-1}$), while Inceptisols and Andisols in the west had a comparable magnitude of topsoil SOC loss (−0.5 to −1.8 Mg C ha^{-1} $year^{-1}$); (b) Mollisols and Alfisols in the Central Plains sites were susceptible to significant SOC loss under farming and grazing; (c) Runoff/erosion and leaching potential, vertical translocation, and mineral sorption were the most important factors controlling SOC variation across the NEON sites. Our work could be used to parameterize ecosystem models simulating SOC change.

Plain Language Summary We estimated the 30-year soil organic carbon (SOC) change in topsoil/A horizon and subsoil/B horizon at National Ecological Observatory Network (NEON) sites based on their soil measurements to identify where, in which soil type, and under which land-use change scenario large SOC increase and/or decrease occurred. Within each eco-climatic domain, the soil plots where soil samples were taken were categorized into different land-cover subgroups from the remote sensing images over 30 years. By controlling the eco-climatic domain and the soil type, the SOC change for each land-use change scenario was estimated. In order to understand the mechanisms of SOC change, we modeled the SOC concentrations in both topsoil and subsoil with their environmental and soil factors. We found that most NEON sites presented SOC loss over the 30 years and more prominently in the topsoil. Under the land-use change scenario ofconverting natural vegetation to croplands and pastures, there will be significant SOC loss after 30-year of cultivation and grazing. Soil processes such as runoff/erosion and leaching, vertical translocation, and mineral sorption determine carbon variation across plots.

1. Introduction

Soil plays an important role in the global carbon cycle as it is the largest terrestrial carbon sink containing more carbon than the atmosphere and biosphere combined (Jobbágy & Jackson, 2000). The soil organic carbon (SOC) stock in the top 1 m has been estimated to be about 1,500 Pg C with considerable variations ranging from 504 to 3,000 Pg across data products and estimates due to the differences in sampling period, intensity and spatial resolution of the soil profile databases, and differences in estimation approaches (Scharlemann et al., 2014; Tifafi et al., 2018). The size of SOC stock also depends on the soil depth, sampling to greater depths generally result in larger SOC stock estimation when deep carbon pools have been included particularly in the tundra and tropics (Jobbágy & Jackson, 2000; Page et al., 2011; Tarnocai et al., 2009). Soil carbon sequestration has been proposed

Writing – review & editing: Jie Hu, Alfred E. Hartemink, Ankur R. Desai, Philip A. Townsend, Rose Z. Abramoff, Zhe Zhu, Debjani Sihi, Jingyi Huang

to mitigate global warming by off-setting part of the carbon dioxide emission from fossil fuel burning and cement production (Lal, 2004). In the USA, following the Growing Climate Solutions Act (S.1251), government and industry are in the process of trading soil-sequestered carbon as a commodity between farmers, ranchers, and corporations.

However, the potential of soil carbon sequestration in cropland and pasture may be overstated as the restoration of carbon may require increased fertilizer production and be accompanied by greenhouse gas emissions from irrigation, mining, and manure application (Amundson & Biardeau, 2018; Lugato et al., 2018; Schlesinger & Amundson, 2019). Moreover, protocols and management efforts providing this capability are highly dependent on the local climatic and edaphic conditions. To evaluate the feasibility and efficacy of soil carbon sequestration in different ecosystems, quantitative estimation and monitoring of SOC stocks and changes are required to back up the above-mentioned initiatives (Gurney & Shepson, 2021).

Previous studies have found that the input and output of SOC are influenced by human-induced changes including global climate change, land cover and land use change (LCLUC), and management activities such as forest harvesting, cropland tillage, and pasture grazing (Erb et al., 2017; Smith et al., 2016; Sun et al., 2020; Tong et al., 2020). A large amount of SOC loss (more than 42% of the initial SOC pool) has been reported in agricultural ecosystems and wetlands of the USA due to intensive human activities (Lal, 1999; Nahlik & Fennessy, 2016). In contrast, substantial SOC gain has (13–21 Tg C $year^{-1}$) been found in the USA forests after reforestation from croplands (Caspersen et al., 2000; Nave et al., 2018). Besides the human-induced changes, soil carbon sequestration could also be affected by soil properties such as texture and pore size, and soil forming factors that are used to define Soil Taxonomy (Huang & Hartemink, 2020; Kravchenko et al., 2019; Luo et al., 2021). Across eco-climatic domains, different soil types have different carbon sequestration potential determined by the balance of all the soil forming factors including climate, organic input, topography, parent material, and soil age (Jenny, 1994; Wiesmeier et al., 2012). Within the same eco-climatic domain, the SOC change in response to LCLUC may be dominantly controlled by the soil type-specific characteristics (e.g., the content and type of clays) (Wiesmeier et al., 2015). Importantly, studies suggest carbon sequestration potential largely depends on the proximity of a given soil to its carbon saturation, which is the upper limit of SOC storage affected by the capacity for mineral sorption at a given level of organic input (Six et al., 2002; Wiesmeier et al., 2014). Recently, a study based on 1,144 globally distributed soil profiles showed a large undersaturation of mineral-associated carbon especially in the deep soil of agricultural ecosystems (Georgiou et al., 2022). Because SOC can still increase and be maintained to a new steady state when inputs are increased, carefully designed experiment studying a series of input versus carbon accrual in the same soil is needed to determine the carbon saturation. Therefore, knowledge gaps remain regarding the location, depth, and quantity of potential carbon sequestration across different eco-climatic regimes, land cover types, and soil types in the USA.

Over the last decades, various carbon cycle models have been developed to predict soil carbon cycle dynamics under different Intergovernmental Panel on Climate Change (IPCC) climate projections and investigate the effects of climate change and human activities on SOC change. Large SOC loss has been reported under projected climate change in the continental United States (CONUS), and soil internal factors (e.g., soil type and soil drainage) have been found to be important controls of SOC stock prediction (Gautam et al., 2022; Gonçalves et al., 2021). Recently, explicit microbial and mineral interactions have been incorporated into models that largely improve the prediction of carbon stocks and dynamics (Abramoff et al., 2022; Sulman et al., 2014; Wang et al., 2013; Wieder et al., 2014). Additionally, a few depth-explicit soil carbon cycle models (Ahrens et al., 2015, 2020; Braakhekke et al., 2011; Camino-Serrano et al., 2018; Nakhavali et al., 2021; Yu et al., 2020) have investigated physicochemical processes like soil erosion and leaching. Despite their finding that a multi-layer representation of the soil profile significantly constrains the SOC stock estimation, most of the carbon cycle models primarily focus on the microbial-active topsoil, which often represents a depth of less than 30 cm. Furthermore, most models estimate SOC stock based on pre-determined depth increments which could be biased by the change in bulk density, different thickness and pedogenic development of the specific diagnostic horizon among different soil types (Ellert & Bettany, 2011; Gifford & Roderick, 2003; Wendt & Hauser, 2013).

Carbon cycle models are often calibrated by controlled-environment lab experiments and/or long-term field monitoring data from eddy covariance flux towers, CO_2 enrichment and warming experiments (McPartland et al., 2019; Wilson et al., 2016) but these observations are generally not distributed across different eco-climatic domains and different land cover types. Given these research gaps, this study applied the space-for-time substitution method to

field-based soil observations of the National Ecological Observatory Network (NEON) to estimate SOC change for different LCLUC scenarios over 30 years at the NEON soil plots. The goal of NEON was to sample across eco-climatic gradients relevant for answering questions about grand challenges in macrosystems ecology. We aim to estimate SOC change at the NEON sites, based on the existing design of NEON, to understand how soil carbon changes varies across eco-climatic gradients, to the extent that our method and NEON's predetermined soil sampling scheme allows us to. But we do not aim to extrapolate the SOC change estimation from NEON soil plots to the whole USA. Topsoil (A horizon) and subsoil (B horizon) SOC changes were calculated for each land-use change scenario while controlling for soil order and eco-climatic domain. Following the SOC change estimation using space-for-time substitution, Structural Equation Modeling was utilized to model the SOC spatial variation and to investigate the controls of environmental and soil internal factors on SOC change in low-SOC and high-SOC soils.

To the best of our knowledge, this study is the first continental-scale, long-term estimation of SOC change for both topsoil and subsoil in the USA. We address the following questions: (a) how has SOC changed over the past 30 years under different land-use change scenarios across eco-climatic domains at NEON soil plots in the USA? (b) Within the same eco-climatic domain, which soil order has the largest SOC decrease/increase in response to LCLUC in topsoil and subsoil? (c) What are the driving factors controlling SOC variation across soil orders and depths?

Our hypotheses are: (a) SOC will increase under natural vegetation over 30 years but decrease under all scenarios of land-use change (e.g., converting natural vegetation into pasture or cropland) due to the reduced C inputs. (b) Younger soils (e.g., Inceptisols) in water-sufficient regions have a greater carbon sequestration potential compared to well-developed (e.g., Ultisols) and/or near carbon-saturated (e.g., Mollisols) soils in water-limited regions. (c) SOC variations are dominantly controlled by soil physicochemical properties and processes including soil pH, mineral sorption, and runoff and/or leaching.

2. Materials and Methods

We first introduce the study areas and the soil plots (Section 2.1) and the NEON soil data including the Soil Taxonomy and measurements of soil physiochemical properties at soil plots (Section 2.2). Then descriptions about the environmental datasets characterizing the climate (Section 2.3.1), plant functional type (Section 2.3.2), and topography (Section 2.3.3) at soil plots are presented. The method of LCLUC detection using remote sensing time series is described in Section 2.3.4. After determining the land cover subgroups of each soil plot based on the total number of detected LCLUC, the space-for-time substitution targeting soil-order- and horizon-specific SOC change estimation due to LCLUC is described in Section 2.4. Finally, the structural equation modeling approach exploring the controlling factors of SOC spatial variation across NEON sites is described in Section 2.5. The flow chart of our data analysis is shown in Figure 1.

2.1. Study Areas

NEON contains 20 eco-climatic domains that cover the contiguous USA, Alaska, Hawaii, and Puerto Rico (Figure 2). Boundaries of NEON domains were created by NEON staff from a combination of multivariate analysis and ecological expertise based on geographic and environmental similarity (Hargrove & Hoffman, 2004; Schimel et al., 2007). Each NEON domain generally consists of two to three terrestrial sites, and 10–26 soil plots were surveyed and sampled in each site (Nave et al., 2021). In this study, a total of 715 soil plots were retained that have measurements of soil physical and chemical properties for both topsoil (A horizon) and subsoil (B horizon).

2.2. Soil Data

Soil samples were collected by diagnostic horizon across all the NEON sites by NEON staff and NRCS between 2015 and 2018. The soil samples collected from a total of 715 soil plots were used in this study. Later, the soil samples were grouped by the eco-climatic domain, soil order, and land-cover subgroup (Section 2.3.4) to conduct the SOC change estimation. A total of 85 (39 topsoil, 46 subsoil) grouped soils were retained, the mean value and standard deviation of the SOC for each grouped soil are provided in Data Set S1. For example, one of the 85 grouped soil is A-D01-Inceptisol-R (the first row in Data Set S1), which contains eight topsoil samples of

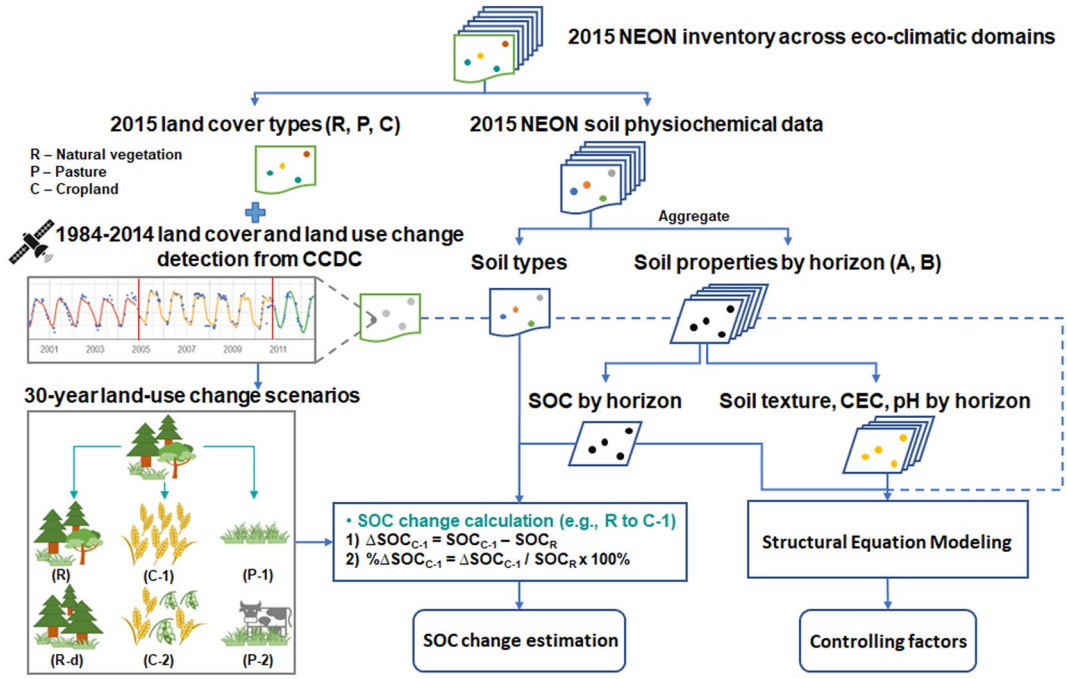

Figure 1. Flow chart of the data analysis.

Inceptisols collected from domain D01 with the land-cover subgroup of reference natural vegetation. We assumed that SOC content remained unchanged during the sampling period (3 years) but will have changed over 30 years due to LCLUC. Soil data used in this study contain Soil Taxonomy description, soil particle size fractions (silt, sand, and clay content), soil organic carbon (SOC), bulk density (Db), pH, and cation exchange capacity (CEC). All the soils were analyzed at the Kellogg Soil Survey Laboratory in Lincoln, NE (Soil Survey Staff, 2014). Because soil samples were taken by each diagnostic horizon, soil properties at different horizons were aggregated

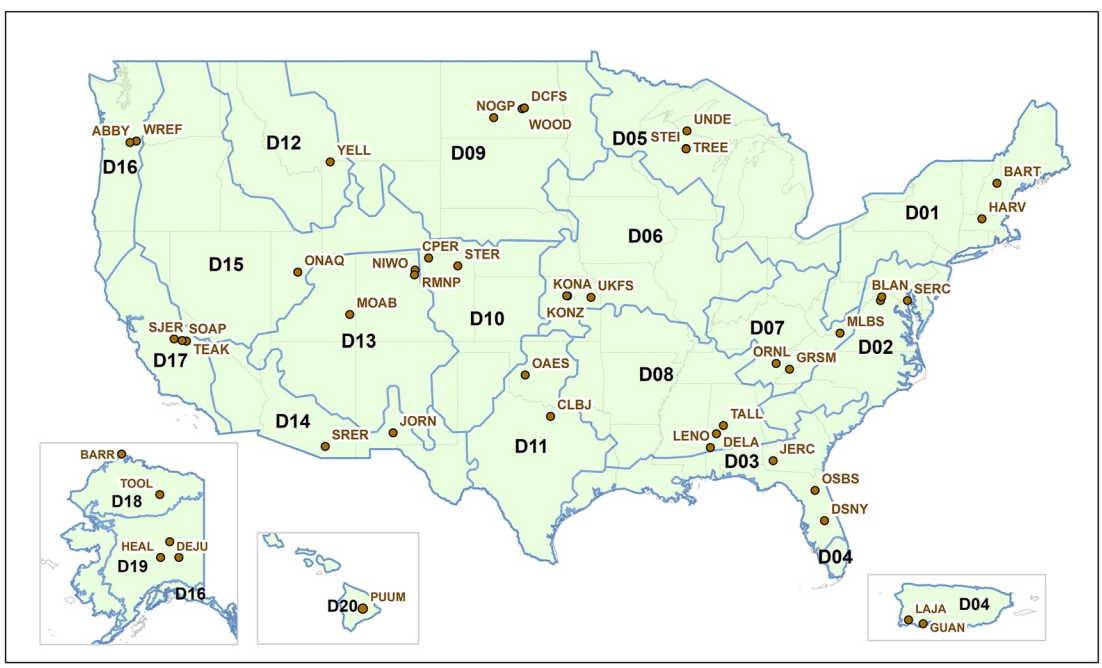

Figure 2. NEON Terrestrial Field Sites Map. List of terrestrial field sites with coordinates acquired from the NEON website (https://www.neonscience.org/field-sites/explore-field-sites).

by their master horizon (A and B) by weighted averaging based on the corresponding thickness of the soil layer. The thickness of A horizon samples ranges between 3 and 94 cm and the thickness of B horizon samples ranges between 7 and 187 cm depending on the soil type. Details about laboratory analyses are given in Text S1 in Supporting Information S1. Statistical summary about the thickness and bulk density of A and B horizon for the soil plots classified into each land-cover subgroup (Section 2.3.4) were provided in Data Set S2.

2.3. Environmental Datasets

A combination of ground observations and laboratory analysis of soil and vegetation properties with remote sensing data products were used to characterize the site information and soil variabilities. Details of the ancillary datasets and the distribution of environmental variables at NEON domains were given in Supporting Information S1 (Table S1 and Text S2).

2.3.1. Climate and Net Primary Production Data

Minimal and maximal annual temperature and mean annual precipitation were calculated from the TerraClimate data set (Abatzoglou et al., 2018) with a temporal coverage from 1984 to 2014 and a 4.6-km spatial resolution. NPP (net primary production) product from Landsat was also extracted at the NEON soil plots within CONUS. The climatic and NPP data were extracted to the pixels where the soil plots were located. The time period and length was selected to cover the duration of Landsat missions (see Section 2.3.4) and represent environmental conditions before soil samples were collected from the NEON sites (see Section 2.2). These climate records were used to characterize the climatic gradients across the soil study plots and used as covariates in the Structural Equation Model (SEM) (Grace, 2006) to quantitatively investigate the influence of climate variables on SOC variation (see details in Section 2.5). The distribution of climatic variables and NPP for the studied soil plots is provided in Supporting Information S1 (Figure S1).

2.3.2. MODIS Land Cover Product

The global and yearly MODIS Land Cover product (MCD12Q1 V006) (Friedl & Sulla-Menashe, 2019) for the year 2015 was processed to characterize the plant functional type of each eco-climatic domain by extracting the pixel value of each soil plot (1 m × 1 m) within a specific domain and summarizing the plant functional types that appeared in that domain. The product has a pixel resolution of 500 m. It consists of 12 different plant functional types ranging from Evergreen Needleleaf Trees, Deciduous Broadleaf Trees, Shrub, Croplands, to Permanent Snow and Ice.

2.3.3. National Elevation Data Set

The 1/3rd arc-second (∼10 m) Digital Elevation Models (DEM) provided by USGS (2020) were downloaded as the original DEM for the NEON sites and then processed using the System for Automated Geoscientific Analyses-Geographic Information System (SAGA-GIS) (Conrad et al., 2015) to derive 14 terrain parameters including slope, aspect, and topographic position index (TPI). These 14 parameters along with the original DEM were used to represent the local topography for our study sites.

2.3.4. Landsat Surface Reflectance and Land Change Detection

Remote sensing data archives acquired by Landsat 5, 7, and 8 satellites (Wulder et al., 2016) were extracted on NEON soil plots over a continuous period of 1984–2014 from the Google Earth Engine (GEE) platform (Gorelick et al., 2017). Landsat Collection 1.0 Tier 1 level-2 surface reflectance data were used as the major remote sensing input. The advantage of using surface reflectance data from GEE is that they have previously been atmospherically corrected and also pre-processed by masking clouds, shadows, water, and snow (Foga et al., 2017; Schmidt et al., 2013; Vermote et al., 2018; Zhu & Woodcock, 2012; Zhu et al., 2015). Given the limited lifespan of the Landsat missions, we limited our study to this time frame to quantify the total number of LCLUC during this period (1984–2014) before the start of soil data collection in the year 2015 (NEON, 2020).

After acquiring the Landsat surface reflectance time series for each soil plot, the Continuous Change Detection and Classification (CCDC) algorithm implemented on GEE was used to detect the time and number of LCLUC over 1984–2014 (Zhu & Woodcock, 2014; Zhu et al., 2015). Essentially this algorithm utilized all the spectral bands of the Landsat time series and modeled the dynamics of surface reflectance by fitting the long-term trend. The seasonal variations of surface reflectance caused by vegetation phenology and solar angle difference were

modeled and removed by the harmonic time series thus only the "breakpoint" where LCLUC occurred would be picked up. By setting the chi-square change probability as 0.99 and the consecutive number of observations required to flag a change or breakpoint as 3, only an abrupt change of land surface (e.g., deforestation, agricultural expansion and intensification, floods, and fire) between two stable land cover segments was recognized as a breakpoint. Spectral bands of B1-5 and B7 in Landsat 5 TM and Landsat 7 ETM+, and B2-7 in Landsat 8 OLI have been specified with the "breakpointBands" argument as input due to their consistent wavelengths, and later used for breakpoint detection of the continuous collection of images. The number of breakpoints/LCLUC detected by the CCDC algorithm over 30 years in addition to the current land cover type were then used to partition the NEON soil plots into six land-cover subgroups for each soil order within the same eco-climatic domain. Among them are reference (R) and disturbed reference (R-d) in natural ecosystems, moderately disturbed (P-1) and intensively disturbed pastures (P-2), and moderately disturbed (C-1) and intensively disturbed croplands (C-2). Soil plots classified as R-d, P-2, and C-2 have a larger number of breakpoints compared to R, P-1, and C-1, respectively. Details about the land-cover subgroups and their distribution in each domain can be found in Tables S2 and S3, Text S3, and Figure S2 in Supporting Information S1.

We used the CCDC algorithm to compare the reference (R) soil versus changed (R-d, P-1, P-2, C-1, C-2) soil instead of detecting the magnitude of land use change. More field survey data covering different levels of land use change need to be collected to fully understand the effect of the magnitude of land use change on SOC. Meanwhile, a sensitivity analysis of the CCDC algorithm was performed and provided in Supporting Information S1 (Text S4, Figures S3, and S4). The patterns of SOC change based on the sensitivity analysis were comparable when different parameters (e.g., chi-square change probability, consecutive number of observations required to flag a breakpoint) values of the CCDC algorithm were used, suggesting the land-cover subgroup classification generated from CCDC was reliable.

2.4. Space-For-Time Substitution

The space-for-time substitution method was employed to study the effects of LCLUC on SOC change due to the lack of long-term co-located observations of SOC contents across the USA. This method assumes that the drivers of spatial gradients of a variable (e.g., biodiversity, SOC) also drive temporal changes in that variable (Blois et al., 2013; Pickett, 1989). It is commonly used in ecological studies and has been applied to map temporal changes of SOC and study the driving factors of SOC change based on empirical models (Adhikari et al., 2019; Bonfatti et al., 2016; Tugel et al., 2005; Waring et al., 2014).

We assume that, for a specific soil (same soil order and horizon) within the same eco-climatic domain, the difference in the mean SOC concentrations between the reference (R) and the five disturbed land-cover subgroups (R-d, P-1, P-2, C-1, C-2) in 2015 is equal to the SOC concentration change over 30 years under five land-use change scenarios. Although there could be over- and/or under-estimation of the SOC change, we are trying to provide a baseline trend of the SOC change under different LCLUC scenarios, of which we believe the direction of most SOC change estimations would not be altered. The five land-use change scenarios are R being converted into (a) R-d, (b) P-1, (c) P-2, (d) C-1, and (e) C-2 in 1984, respectively. Thus mean SOC concentrations (g C kg^{-1}) were first calculated for each soil order and horizon under different land-cover subgroups within each domain. Those SOC concentrations aggregated with a sample size of less than 4 were considered not representative of the specific soil and thus excluded. Then the difference in the mean SOC concentrations between the reference and the specific disturbed land-cover subgroups was taken as the absolute SOC change for the corresponding land-use change scenario. Although the 715 soil plots were sampled from 20 NEON eco-climatic domains, several domains ended up with insufficient (<4) soil plots classified into the reference and/or disturbed states which are essential for SOC change estimation, leading to a total of 16 domains with SOC change estimates shown in the results. The statistical significance of each SOC change estimate was also analyzed from a *t*-test to see whether a significant difference existed in the mean SOC concentrations between the reference and the disturbed land-cover subgroups. We also calculated the relative SOC change in percentage as the ratio of the absolute SOC change to the mean SOC concentration in the reference to exclude the effect of initial SOC concentration. To visualize the spatial pattern of SOC change at NEON sites, the absolute and relative SOC change for a specific soil under a specific land-use change scenario was represented as a circle drawn onto each eco-climatic domain. The latitude and longitude of each circle is the average of all the soil profiles used for the SOC change calculation. Circles in D02 Mid Atlantic, D06 Prairie Peninsula, and D08 Ozarks Complex have been moved to avoid overlapping while

remaining in the same domain. Additionally, the SOC change rates (g C kg^{-1} $year^{-1}$) over 30-year period were further calculated by dividing the absolute SOC change by 30. Finally, the SOC change values were compared across soil orders, eco-climatic domains, and LCLUC scenarios to investigate which soil, environment, and LCLUC scenario has more carbon accrual or carbon loss. Tukey mean statistical test (Driscoll, 1996) was used to account for the effect of sample size when comparing the SOC change values across different soil orders and eco-climatic domains.

2.5. Structural Equation Modeling

Structural Equation Modeling (SEM) is a methodology for developing and testing hypotheses about relationships in a system that encompasses different statistical tools for causal analysis (Eisenhauer et al., 2015). The path diagrams of SEM have been used to represent the cause-effect network (Grace, 2006). In this study, we applied SEM to systematically quantify the interrelationships between both edaphic and environmental factors with SOC measured in topsoil (A horizon) and subsoil (B horizon) using the R package "lavaan" (Rosseel, 2012). We first developed the conceptual SEM model based on the soil forming factors that could affect SOC, then calibrated it using the measured SOC, soil physiochemical properties and environmental data.

The conceptual SEM model (Figure S5 in Supporting Information S1) consists of 9 latent variables. Similar to the dependent variables in regression models, the two endogenous latent variables are measured SOC in topsoil and subsoil. The seven exogenous latent variables are grouped as three environmental factors—litter, heat, runoff/erosion and leaching potential, and four edaphic factors—mineral sorption in topsoil and subsoil, and pH in topsoil and subsoil. The litter input was based on multi-year average NPP reflecting the long-term land use, the heat factor (surface energy balance and evaporative demand) was represented by five observed variables—solar radiance, potential evapotranspiration, minimum and maximum annual temperatures, and vapor pressure deficit. Precipitation, topographic position index, and segment/break numbers of LCLUC were used in the model to characterize the runoff/erosion and leaching potential factor. The mineral sorption factor was calculated based on the ratio of clay content to cation exchange capacity (CEC). The latent variables of pH in topsoil and subsoil were depicted by measured soil pH in topsoil and subsoil, respectively.

The ratio of clay content to cation exchange capacity has been used as a surrogate for mineral sorption when detailed information for clay mineral composition is not available (Bloesch, 2012; Pearring, 1968). The clay activity or ability to absorb organic carbon per unit of clay could better represent the effect of mineral sorptions on SOC dynamics compared to the clay content alone. Previous studies have found this surrogate to be more accurate in soils with low SOC content as SOM also contributes to the increase of CEC in soils with high SOC content (Eldridge, 2003). To separate the contribution of SOM and clay sorption to this ratio, we built two SEM models for NEON soil plots, one with low SOC and the other with high SOC.

3. Results

3.1. SOC Changes at NEON

The SOC change estimation was made for the NEON soil study plots under different LCLUC scenarios where soil plots with natural vegetation without LCLUC were converted to those with managed land-cover types. Noting that results in this study should not be directly extrapolated to the rest of USA where samples have not been collected. Figure 3 illustrates the absolute and relative SOC change maps over 30 years in topsoil and subsoil (details provided in Tables S4 and S5 in Supporting Information S1). Significant (p value < 0.05 from t-test) SOC change estimations have been denoted with asterisks next to the underlined labels. In general, there is large carbon loss in both topsoil and subsoil. All the significant SOC change values showed carbon loss, including three Mollisols and one Ultisols in cropland in the topsoil, and two Mollisols in cropland and one Inceptisols in a natural ecosystem in the subsoil. Uncertainty exists in the SOC change results as the rest of the SOC change estimates were not statistically significant. The uncertainty was largely attributed to the NEON sampling design where most of the terrestrial sites are located in natural ecosystems with a limited effect of LCLUC on SOC change. Specifically, a potential SOC increase without a statistical significance in Alaska subsoil was discussed in Supporting Information S1 (Text S5). Among the 16 domains with SOC change estimates, only six of them have soils sampled in managed ecosystems with an accepted sample size (≥ 4) (Figure S2 in Supporting Information S1). Nonetheless, our analysis in general suggests decreasing trend of SOC and revealed statistical uncertainty associated with imbalanced sampling design which needs to be considered when designing carbon monitoring systems.

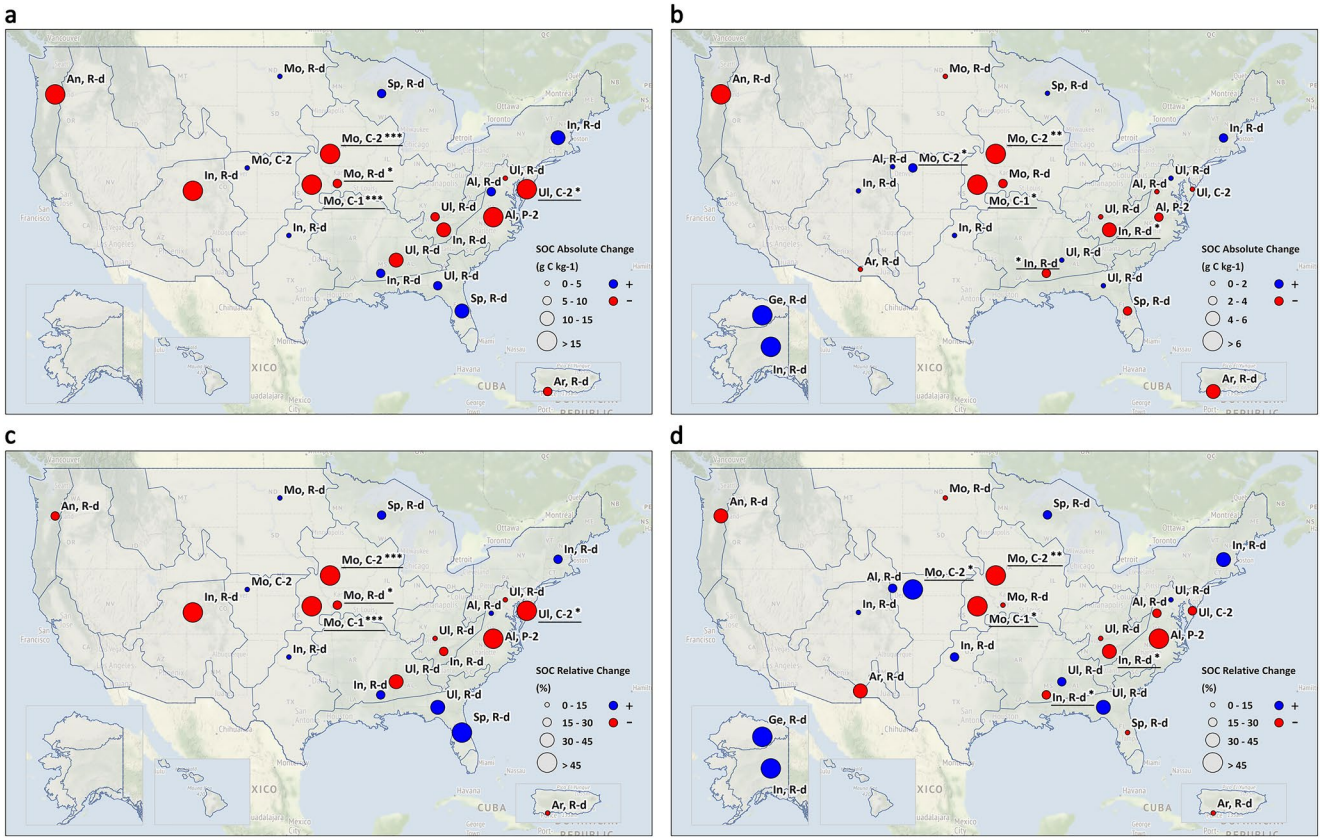

Figure 3. SOC absolute change in topsoil (a) and subsoil (b) (g C kg^{-1}) and relative change in topsoil (c) and subsoil (d) (%) at NEON sites. Blue circles refer to SOC increase, red circles refer to SOC decrease. The first two letters of the label are for the soil order (Al—Alfisols, An—Andisols, Ar—Aridisols, Ge—Gelisols, In—Inceptisols, Mo—Mollisols, Sp—Spodosols, Ul—Ultisols), the last two letters of the label describe the land use change scenario (R-d—reference to disturbed natural vegetation, P-2—reference/disturbed reference to intensively disturbed pasture, C-1—reference/disturbed reference to disturbed cropland, C-2—reference/disturbed reference to intensively disturbed cropland). Notes: Absence of SOC change in topsoil due to limited (<4) topsoil data for soil plots classified as a reference and/or disturbed land-cover subgroup in Alaska. *$p < 0.05$, **$p < 0.01$, ***$p < 0.001$.

The absolute SOC changes in topsoil between 1984 and 2014 ranged from −30.1 g C kg^{-1} (−1.8 Mg C ha^{-1} $year^{-1}$) to +14.9 g C kg^{-1} (+1.2 Mg C ha^{-1} $year^{-1}$) with a median of −6.0 g C kg^{-1} (−0.3 Mg C ha^{-1} $year^{-1}$). Although not all the estimates have statistical significance, a trend of SOC decrease occurred in the mid-latitude regions including disturbed croplands (Ultisols, Mollisols) and pastures (Alfisols) in the eastern domains and disturbed natural vegetation (Andisols, Inceptisols) in the western domains. In comparison, SOC gains were identified in water-sufficient eastern domains in Spodosols and Inceptisols under disturbed natural vegetation (R-d).

Compared to the topsoil, the absolute SOC change in subsoil shifted toward carbon gain ranging from −7.8 g C kg^{-1} (−3.7 Mg C ha^{-1} $year^{-1}$) to +27.5 g C kg^{-1} (+2.7 Mg C ha^{-1} $year^{-1}$) with a median of −0.7 g C kg^{-1} (−0.3 Mg C ha^{-1} $year^{-1}$). Large SOC gains were found in Gelisols in D18 Tundra and Inceptisols in D19 Taiga in Alaska in the land-use change scenario from the reference (R) to disturbed natural vegetation (R-d). However, the changes were not statistically significant due to limited sample size and large spatial heterogeneity in Alaskan soils as revealed by the NRCS data archive (data not shown). The relative change of SOC ranged from −64% to +60% in topsoil and −52% to +72% in subsoil with similar patterns compared to the absolute change of SOC.

3.2. Across-Domain SOC Changes

Inceptisols, Ultisols, and Mollisols have SOC change estimates in more than one domain. The absolute and relative change in SOC of Inceptisols and Ultisols across domains are given in Table 1 in the land use change scenario from the reference (R) to the disturbed reference (R-d) under natural vegetation, and for Mollisols in Table 2 in the land use change scenario converting natural vegetation (R or R-d) to intensively disturbed cropland

Table 1
Soil Organic Carbon (SOC) Change and Rate of Change for Inceptisols and Ultisols Across Domains Under the Land-Use Change Scenario of Converting Natural Vegetation to Disturbed Natural Vegetation (R to R-D)

Soil order	Domain ID	Domain name	n	SOC_{abs} g C kg^{-1}	SOC_{rela} %	NPP g C m^{-2}	MAP mm	T_{min} °C	T_{max} °C	PFT
Inceptisols					*A horizon*					
	D01	Northeast	6	14.4^{b}	29^{a}	762.7^{b}	1156^{b}	-12^{c}	27^{a}	DBT
	D08	Ozarks Complex	11	5.0^{ab}	20^{a}	741.1^{b}	1432^{a}	1^{b}	34^{b}	DBT
	D11	Southern Plains	8	0.8^{ab}	5^{a}	248.3^{c}	724^{c}	-4^{a}	36^{b}	Grass
	D07	Appalachian and Cumberland Plateau	9	-11.2^{ab}	-16^{a}	922.1^{a}	1292^{ab}	-5^{a}	29^{a}	DBT
	D13	Southern Rockies and Colorado Plateau	5	-30.1^{a}	-49^{a}	222.3^{c}	437^{d}	-12^{c}	28^{a}	Grass and ENT
					B horizon					
	D19	Taiga	24	6.2^{b}	59^{b}	-	306^{e}	-25^{d}	21^{d}	ENT and DBT
	D01	Northeast	7	2.6^{ab}	37^{ab}	797.4^{b}	1152^{f}	-12^{c}	27^{ac}	DBT
	D11	Southern Plains	8	1.9^{ab}	22^{ab}	248.3^{c}	724^{c}	-4^{a}	36^{b}	Grass
	D13	Southern Rockies and Colorado Plateau	7	0.7^{ab}	11^{ab}	293.1^{c}	475^{d}	-13^{c}	26^{c}	Grass and ENT
	D08	Ozarks Complex	11	-2.6^{a}	-26^{ab}	741.1^{b}	1432^{b}	1^{b}	34^{b}	DBT
	D07	Appalachian and Cumberland Plateau	12	-4.9^{a}	-33^{a}	906.2^{a}	1291^{a}	-5^{a}	29^{a}	DBT
Ultisols					*A horizon*					
	D03	Southeast	19	7.6^{a}	44^{a}	691.0^{a}	1294^{a}	3^{a}	34^{a}	DBT and EBT
	D02	Mid-Atlantic	15	-3.6^{ab}	-13^{b}	799.7^{b}	1076^{d}	-4^{b}	31^{c}	DBT
	D07	Appalachian and Cumberland Plateau	14	-6.0^{b}	-14^{b}	838.7^{b}	1244^{b}	-4^{b}	30^{b}	DBT
	D08	Ozarks Complex	25	-11.6^{b}	-33^{b}	713.4^{a}	1363^{c}	0^{c}	33^{a}	DBT
					B horizon					
	D08	Ozarks Complex	24	0.9^{a}	21^{a}	708.9^{a}	1360^{b}	0^{c}	33^{a}	DBT
	D03	Southeast	14	0.8^{a}	43^{a}	700.0^{a}	1294^{a}	3^{a}	34^{a}	DBT and EBT
	D02	Mid-Atlantic	15	0.3^{a}	11^{a}	799.7^{b}	1076^{c}	-5^{b}	31^{c}	DBT
	D07	Appalachian and Cumberland Plateau	16	-1.2^{a}	-15^{a}	834.6^{b}	1254^{a}	-4^{b}	30^{b}	DBT

Note. SOC_{abs}—absolute change of soil organic carbon, SOC_{rela}—relative change rate of soil organic carbon, SOC_{mean}—mean value of soil organic carbon, NPP—net primary production, MAP—mean annual precipitation, T_{min}—annual average minimum temperature, T_{max}—annual average maximum temperature, PFT—the dominant plant functional type, DBT—Deciduous Broadleaf Trees, ENT—Evergreen Needleleaf Trees, EBT—Evergreen Broadleaf Trees. The superscript letters above values represent the result of the Tukey test for pairwise mean comparisons, different letters represent the means differ significantly ($p < 0.05$) between the pair.

(C-2) under agricultural management. Complete lists of SOC change in other soil orders under different land use change scenarios are shown in Tables S4/S5 in Supporting Information S1 but not presented here since they do not have SOC change estimates in more than one domain for cross-domain comparison.

In topsoils of Inceptisol, the largest SOC increase was found in D01 Northeast and the largest SOC decrease was found in D13 Southern Rockies and Colorado Plateau (Table 1). As for the subsoil, the largest SOC increase was +6.2 g C kg^{-1} (+1.0 Mg C ha^{-1} $year^{-1}$) in D19 Taiga, whereas the largest SOC decrease (−4.9 g C kg^{-1}, –0.9 Mg C ha^{-1} $year^{-1}$) in subsoil was found in D07 Appalachian and Cumberland Plateau.

For Ultisol topsoils, SOC had the largest increase in D03 Southeast but decreased the most in D08 Ozarks Complex. In the subsoil, SOC slightly increased in D08 Ozarks Complex but decreased in D07 Appalachian and Cumberland Plateau.

Inceptisols and Ultisols showed opposite SOC changes in D08 Ozarks Complex regarding different horizons, whereas SOC tended to decrease in D07 Appalachian and Cumberland Plateau regardless of soil orders and

Table 2
Soil Organic Carbon (SOC) Change Rate for Mollisols Across Domains Under Land Use Change Scenario of Converting Natural Vegetation or Disturbed Natural Vegetation to Cropland (R/R-D to C-2)

Soil order	Domain ID	Domain name	*n*	SOC_{abs} g/kg	SOC_{rela} %	NPP g C m^{-2}	MAP mm	T_{min} °C	T_{max} °C	PFT
Mollisols					*A horizon*					
	D10	Central Plains	5	1.1***	11***	440.4***	428***	−11***	32***	Grass
	D06	Prairie Peninsula	11	−25.6***	−59***	664.3***	885***	−9***	33***	Grass and Cereal Croplands
					B horizon					
	D10	Central Plains	5	2.8***	75***	Same as above				
	D06	Prairie Peninsula	11	−7.8***	−52***					

Note. SOC_{abs}—absolute change of soil organic carbon, SOC_{rela}—relative change rate of soil organic carbon, SOC_{mean}—mean value of soil organic carbon, NPP—net primary production, MAP—mean annual precipitation, T_{min}—annual average minimum temperature, T_{max}—annual average maximum temperature, PFT—the dominant plant functional type, DBT—Deciduous Broadleaf Trees, ENT—Evergreen Needleleaf Trees, EBT—Evergreen Broadleaf Trees. *$p < 0.05$, **$p < 0.01$, ***$p < 0.001$.

horizons. Under the same land use change scenario from reference (R) to disturbed reference (R-d), both Inceptisols and Ultisols have either increased or decreased SOC in topsoil and subsoil, while weakly developed, young soils (Inceptisols) have a larger magnitude of SOC change compared to fully-developed, mature soils (Ultisols), indicating a greater potential of soil carbon sequestration in Inceptisols.

In contrast with Inceptisols and Ultisols that have SOC change estimates in more than three different domains, Mollisols in the land use change scenario from natural vegetation to cropland were only identified in two domains (Table 2) due to the NEON sampling design where most of the terrestrial sites are located in natural ecosystems. The SOC was moderately increased in both topsoil and subsoil in D10 Central Plains but substantially decreased in topsoil and subsoil in D06 Prairie Peninsula.

3.3. Within-Domain SOC Changes

A comparison of SOC change between Ultisols and other soils (Alfisols, Inceptisols, and Spodosols) within the same domain in the land use change scenario from the reference (R) to the disturbed natural vegetation (R-d) is given in Table 3. Only the results with statistical significance were included. Ultisols decreased in topsoil SOC across all domains except D03 Southeast, and SOC either decreased or remained unchanged (SOC absolute change <+1 g C kg^{-1}) in the subsoil. In contrast, other soil orders such as Alfisols and Inceptisols have increased SOC in topsoil but not subsoil. Regardless of the direction of SOC change (increase or decrease), fully-developed Ultisols showed a smaller magnitude of SOC change in concentration compared with other soil types within the same eco-climatic domain and land use change scenario.

3.4. SEM Results for NEON Soil Plots

Two SEM models were built for NEON soil plots with low SOC and high SOC, respectively. As shown in Figure 4, the orange lines with arrows demonstrate the path starting from exogeneous variables pointing toward endogenous variables. Solid arrows represent positive paths and dashed arrows represent negative paths. The thickness of the arrows reflects the magnitude of the standardized path coefficients. Non-significant paths ($P > 0.05$) were excluded and not shown. The numbers adjacent to the paths were the path coefficient of different environmental and edaphic factors. Each path coefficient quantifies the effect of that specific factor on SOC variation across soil plots in the given model.

Both models showed a significant effect of mineral sorption on the SOC variation across studied soil plots. Within each model, the sorption effect in the subsoil was greater than that in the topsoil. Specifically, the sorption effect had a coefficient of 0.33 in the subsoil and 0.11 in the topsoil for the low-SOC model (Figure 4a). While for the high-SOC model (Figure 4b), the sorption effect coefficients were 0.48 in the subsoil and 0.25 in the topsoil.

For the low-SOC model (Figure 4a), runoff and/or leaching had the most dominant effect on the subsoil SOC variation with the largest coefficient of 0.59. In addition, the topsoil SOC itself also had a significant effect on

Table 3
Comparison of Soil Organic Carbon (SOC) Change Between Ultisols, Alfisols, Spodosols, and Inceptisols Within the Same Domain Under the Land Use Change Scenario of Converting Natural Vegetation to Disturbed Natural Vegetation (R to R-D)

Domain	Soil order	*n*	SOC_{abs} g/kg	SOC_{rela} %	NPP g C m^{-2}	DEM m	Sand %	Silt %	Clay %	CEC cmol (+)/kg	pH	Db g/cm^3
D02 Mid-Atlantic						*A horizon*						
	Alfisols	8	6.0	13	732.5	340***	18***	55***	27***	20*	5.7*	1.3
	Ultisols	15	−3.6	−13	799.7	50***	48***	36***	16***	13*	5.0*	1.4
						B horizon						
	Alfisols	8	−1.7*	−26*	732.5	340***	15***	44**	41**	11	5.5*	1.5**
	Ultisols	15	0.3*	11*	799.7	50***	43***	29**	28**	14	4.9*	1.6**
D03 Southeast						*A horizon*						
	Spodosols	7	14.9	60	600.8*	22***	93***	5***	1***	10	4.0***	1.4
	Ultisols	19	7.6	44	691.0*	41***	82***	13***	5***	7	5.3***	1.5
						B horizon						
	Spodosols	6	−2.9*	−14	600.8*	23***	94***	4***	2***	7**	4.0***	1.5
	Ultisols	14	0.8*	43	691.0*	41***	67***	12***	20***	3**	5.5***	1.6
D07 Appalachian and Cumberland Plateau						*A horizon*						
	Inceptisols	9	−11.2	−16	922.1*	558	43	38	19	18*	4.6	1.1
	Ultisols	14	−6.0	−14	838.7*	452	38	43	20	14*	4.9	1.1
						B horizon						
	Inceptisols	9	−4.9*	−33	922.1*	558	40	40	20*	10	4.8	1.4**
	Ultisols	14	−1.2*	−15	838.7*	452	32	39	29*	9	4.7	1.5**
D08 Ozarks Complex						*A horizon*						
	Inceptisols	11	5.0**	20*	741.1	17***	19	40	41**	29***	5.3	1.5
	Ultisols	25	−11.6**	−33*	713.4	51***	34	39	27**	15***	5.2	1.4
						B horizon						
	Inceptisols	11	−2.6***	−26*	741.1	17***	30	33	37	21*	5.0	1.6
	Ultisols	24	0.9***	21*	713.4	51***	30	37	32	12*	5.3	1.5

Note. SOC_{abs}—absolute change of soil organic carbon, SOC_{rela}—relative change rate of soil organic carbon, SOC_{mean}—mean value of soil organic carbon, DEM—digital elevation model, CEC—cation exchange capacity, TPI—topographic position index, Db—bulk density, NPP (net primary production) was estimated from Landsat data, used here for illustration. Due to the lack of oven-dried bulk density in D03 from the NEON data set, bulk density data from SoilGrids 2.0 was used and presented for D03 soils here. *$p < 0.05$, **$p < 0.01$, ***$p < 0.001$.

the subsoil SOC. In contrast, runoff and/or leaching did not influence the SOC variation significantly in the high-SOC model (Figure 4b).

4. Discussions

4.1. Constraints of Carbon Sequestration at the NEON Sites

4.1.1. Limited Carbon Sequestration Potential in Cropland and Pasture

Cropland and pasture without good management and/or land recovery have limited carbon sequestration potential because of the low plant diversity, frequent harvest and grazing, and intense soil compaction and erosion which fundamentally deprives the soil of carbon input (Lal, 2003; Post & Kwon, 2000; Yang et al., 2019). Under the land-use change scenario of converting natural vegetation to managed ecosystems, carbon sequestration indicated by positive SOC change estimate was only observed in D10 Central Plains possibly due to improved management in the cropland. No-till management in croplands has been introduced since 1985 at the NEON STER (North Sterling) terrestrial site in D10, which could lead to SOC increase compared to conventional tillage. More importantly, greater inputs from the vegetation because of improved management such as fertilization and irrigation

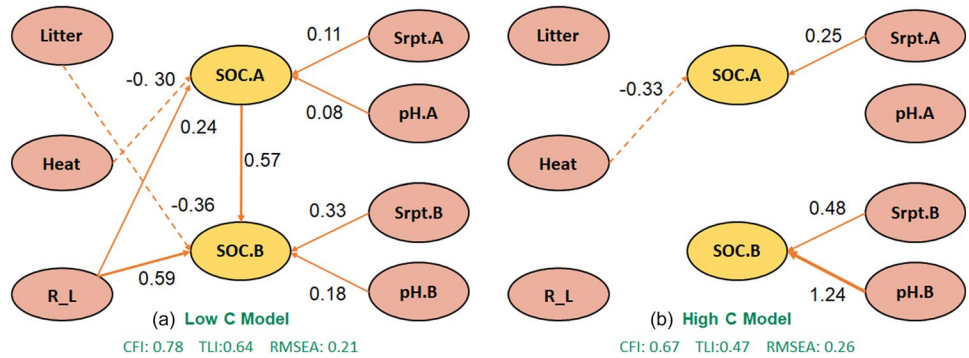

Figure 4. SEM low-SOC (a) and high-SOC (b) model of the effects of environmental (Litter, Heat, and R_L) and edaphic (Srpt.A, Srpt.B, pH.A, and pH.B) factors on topsoil and subsoil SOC variation fitted using data across NEON soil plots. Litter factor was based on multi-year average net primary production reflecting long-term land use. Heat factor was represented by five observed variables—solar radiance, potential evapotranspiration, minimum and maximum annual temperatures, and vapor pressure deficit. Precipitation, topographic position index, and segment/break numbers of land-cover and land-use change derived from CCDC (Continuous Change Detection and Classification) were used to characterize the runoff/erosion and leaching potential factor (R_L). The mineral sorption factor of topsoil (Srpt.A) and subsoil (Srpt.B) was calculated based on the ratio of clay content to cation exchange capacity for each soil layer. pH.A: pH of topsoil; pH.B: pH of subsoil. The CFI (comparative fit index), TLI (Tucker Lewis index), and RMSEA (root mean square error of approximation) are fit indices of the model.

may contribute to the SOC accrual in the cropland compared to the natural system. All other cropland (Mollisols in D06, Ultisols in D02) and pasture soils (Alfisols in D02) showed large amounts of SOC loss in both topsoil and subsoil.

Improved management such as cover crops, rotation, and residue return may reduce the SOC loss in cropland and pasture but would not always turn the SOC loss into a SOC gain especially when the soil is near carbon saturation (Guillaume et al., 2022; Six et al., 2002; Stewart et al., 2007). For instance, a long-term cropping system trial from silt loam Mollisols in the North Central USA failed to sequester additional carbon from 29 years of improved management practices including reduced tillage, diversified crop rotations with cover crops and legumes, and manure addition (Rui et al., 2022; Sanford et al., 2012). The soils (0–15 cm) had initially 31 g C kg^{-1} at the onset of their study, almost triple the size of the topsoil SOC concentration for reference state Mollisols (10.5 g C kg^{-1}) in D10 Central Plains in our study, suggesting our soils in D10 may be far from carbon saturation. Another study of long-term SOC dynamics conducted in Switzerland also found the initial SOC concentration to be the dominant variable explaining the SOC change rates, and the SOC accumulation rates decrease with increased initial SOC concentration in temperate cropland-grassland systems (Guillaume et al., 2021). Although previous studies have also reported that soils have higher relative carbon sequestration rates with lower initial carbon contents, it has not been tested across eco-climatic domains at a large scale, and the observations tend to be limited in the top 30 cm of the soil profile (Tan & Lal, 2005; Tan et al., 2004).

SOC sequestration in managed ecosystems was only estimated in D10 Mollisols in our study with low carbon stock after 30 years of improved cultivation. Moreover, increasing fertilization, irrigation, and manure application contribute to the increasing emission of greenhouse gases from management activities (Schlesinger & Amundson, 2019; Snyder et al., 2009). Thus, we appeal for caution when considering trading carbon credits by attempting to sequester carbon in cultivated soils.

4.1.2. Limited Carbon Sequestration Potential in Well-Developed Soils

Several major edaphic features contribute to the SOC stabilization; among these are: (a) clay minerals that provide physical protection; (b) sesquioxides (e.g., Fe- and Al-oxides) that control ligand-exchange reactions; (c) cations (e.g., Ca^{2+}) that can form cation-bridges between both negatively charged soil organic matter (SOM) and negatively charged clay minerals; and (d) short order silicates (e.g., allophane) that have van der Waals interactions (Cotrufo et al., 2013; Rasmussen et al., 2018; Shen, 1999).

In well-developed soils such as Ultisols, low adsorption capacity constrains the SOC sequestration since most of the cations have been leached out, in particular from the topsoil. The majority of the limited SOC retention

in the subsoil primarily comes from the ligand-exchange interaction between sesquioxides and SOM (Qichun Zhang et al., 2014). Although accumulated clay could be found in the subsoil, they tend to have low activity with low CEC value and therefore fail to retain large amount of carbon. Previous studies suggest that the types and characteristics of clay minerals (e.g., expandability, surface area, crystalline structure), instead of clay content, have a greater effect on SOC stabilization (Solly et al., 2020; Torn et al., 1997; Wattel-Koekkoek et al., 2001). As the ratio of CEC to clay content partly reflects the types and characteristics of clay minerals through quantifying surface areas per unit of clay, it could be used as a promising proxy indicating clay mineralogy in carbon cycle models when sufficient clay mineral information is not available and the soil is not rich in SOM (e.g., Ultisols). However, it should be noted that such alternative could overestimate the carbon sequestration capacity due to mineral sorption if the soil is SOM rich. Because high amount of SOM would contribute to large value of CEC as well. Besides, less developed soils such as Inceptisols tend to have large range of soil properties which should be considered when using the CEC to clay ratio as a surrogate for mineral sorption (Rasmussen et al., 2018).

Whether a soil is near-saturated or not is also affected by many factors including the ones which are not represented in the soil taxonomy, such as management and disturbance. Furthermore, sequestration potential is dynamic and dependent on organic matter inputs and the climate which are subject to gradual change over time such as intensified interannual variability. Although generalization by soil order is useful for predicting SOC change at some level, within-order variation exists and thus should not be ignored regarding carbon sequestration estimation.

4.1.3. Limited Carbon Sequestration Potential in Water-Limited Regimes

The constraints on carbon sequestration in water-limited regimes derive from both the low vegetation input due to insufficient plant-available water and the high microbial accessibility to SOM. The latter is controlled by processes which reduce the soil aggregate stability, such as the drought-induced soil structure/macro-porosity change (Zhang et al., 2019). Soil moisture was reported to drive 90% of the inter-annual variability in global carbon uptake through the enhanced impact of soil water stress on carbon assimilation due to the feedback between soil and atmospheric dryness (Humphrey et al., 2021). At higher water suction (drier condition), a secondary pool of labile carbon in these organic soils becomes accessible to the microbial community through (a) drying-induced consolidation; (b) loss of macro-porosity; and (c) exposure of SOM isolated by aggregates to air (Kaiser et al., 2015).

Natural ecosystem carbon stock is more constrained by water in dry areas, whereas heat and nutrient resources play a more important role in SOC dynamics in humid areas (Tang et al., 2018). The direction of carbon cycle feedback to climate warming has been reported to be controlled by the water availability as it influences ecosystem productivity (Quan et al., 2019). Our results suggest that carbon sequestration potential in the dry domains is limited in both topsoil and subsoil. The Inceptisols in D13 Southern Rockies and Colorado Plateau showed abundant carbon loss in the topsoil and limited carbon increase in the subsoil. Additionally, the Andisols in D16 Pacific Northwest showed large carbon loss in both topsoil and subsoil. However, these changes were not significant which could be explained by the moderate intensity of LCLUC in natural ecosystems.

4.2. Vertical Translocation, Mineral Sorption, and Leaching Contributed to Subsoil SOC Accrual

Though topsoil has the highest concentration of carbon in the soil profile and is most biologically active, more than half of the SOC is stored below the A horizon as reported by other studies (Jobbágy & Jackson, 2000; Moreland et al., 2021). In the subsoil, the leaching-driven vertical movements (e.g., transport of colloids, particulate organic matter, dissolved organic matter, and microbial biomass) dominantly drive the SOC dynamics which is controlled by the percolation/drainage rate and the physiochemical characteristics of the soil (e.g., mineral sorption and protection due to different pore size and clay mineralogy) (Bruun et al., 2007; Guber et al., 2022; Luo et al., 2019). In the SEM model of the low-SOC soil plots (Figure 4a), the runoff and leaching potential was the most significant driver of SOC variation in the subsoil. Additionally, a significant connection between SOC.A and SOC.B was found in low-SOC soil plots, which suggests that vertical translocation of SOC along the profile could be a dominant source of SOC accrual in the subsurface layer. Furthermore, as illustrated in the SEM models for both low-SOC and high-SOC soil plots (Figure 4), mineral sorption and protection, manifested by the ratio of CEC to clay content, played an important role in SOC stabilization in both A (topsoil) and B (subsoil) horizons. Explicit representation of vertical translocation, sorption and leaching processes may improve the representation of soil carbon for different depths in carbon cycle models.

4.3. Future Work

Due to the selection of NEON terrestrial sites (natural ecosystem dominant), the specific SOC change at each domain may not be representative enough to be applied to other regions and scaled across entire domains. Additional field observations are required to sample these managed ecosystems and include them in the modeling effort. Beyond the NEON soil sampling sites, land use change scenarios can be more complex and dynamic than the one-way conversion from natural vegetation to disturbed natural vegetation, cropland, and pasture mostly considered here. Moreover, the selection of soil plots by NEON was not made with the intent of comparing paired LCLUC plots, and the soil spatial heterogeneity within domain (e.g., D18, D19) and/or soil type was insufficiently represented to support SOC change estimation with statistical significance. We therefore stress the importance of reflecting LCLUC and soil spatial heterogeneity for different soil types in the sampling design, as there is a need for accurate monitoring of SOC dynamics.

Despite the merits of the CCDC algorithm regarding detecting continuous LCLUC, a recently developed algorithm named Continuous monitoring of Land Disturbance (COLD) (Zhu et al., 2020) may eliminate the vegetation regrowth breaks and improve the accuracy of categorizing soil plots into the reference or disturbed subgroups particularly for forest disturbance with relatively small magnitude of change in the surface reflectance spectra. Given its performance of detecting different land disturbance types including harvest, mechanical disturbance, wind, and fire (Zhu et al., 2020), COLD would help to investigate the effect of specific disturbance type on SOC change for future studies and benefit a broader audience for large-scale time series analysis of the environment.

This study assumes that 30-year climate change has a minimal impact than LCLUC by controlling the eco-climatic domain and soil order when estimating the SOC change. We acknowledge the limitation of the space-for-time substitution as other factors such as the increasing temperature and changed precipitation within the 30 years, as well as the legacy effect of LCLUC before 1984 could also influence the SOC dynamics (Li et al., 2022). We used this method as an alternative because neither ground-truth observation nor long-term remote sensing time series were available for use to tease out this legacy effect from our SOC change estimation across eco-climatic gradients at the continental scale. Nonetheless, over the 30 years, both the reference and the changed soil plots have been subject to similar climate change. Since the SOC change estimates in our study were calculated from the difference of measured SOC concentration between the reference and the changed soil plots for a given soil order within the same eco-climatic domain, the climate change effect on SOC change under land-use change scenarios could be largely canceled out. The effect of the same climate change on the SOC could vary between the reference and the changed soil plots, which is controlled by the specific LCLUC scenario. We assume that the 30-year LCLUC has the dominant effect on SOC change, especially at those sites where significant changes have been estimated. Furthermore, our data does suggest significant changes in SOC likely occurred in several regions sampled by the NEON domain. Knowing this change is important for understanding the evolution of the carbon cycle at these sites over the future life of NEON observations.

Advances in carbon cycle models have been made over the decades (Abramoff et al., 2022; Sulman et al., 2018; Wang et al., 2013; Wieder et al., 2015), while limitations remain in the schemes of current models as (a) decomposition has been over-simplified with the assumption of constant soil physicochemical properties; (b) vegetation and human-induced disturbance within the same land cover type has not been well-represented except for harvest and fire in some models including JSBACH (Lasslop et al., 2016) and LPJ-GUESS (Smith et al., 2001); (c) processes like runoff/erosion and leaching-driven vertical translocation of SOC along the profile have been recognized in regional and global studies but not widely used especially in the Coupled Model Intercomparison Project Phase 6 (CMIP6) models (Boysen et al., 2021). Additionally, microbial-mineral interactions were often parameterized by soil properties such as pH, soil texture, and bulk density while ignoring the types and characteristics of clay minerals on mineral sorption especially in the subsoil. Land carbon cycle models could be largely improved if edaphic processes such as runoff/erosion and leaching along the profile were taken into account. Further research is still needed to improve our understanding of mineral-associated SOC in response to LCLUC across soil types and eco-climatic domains, as well as the movement of SOC due to runoff/erosion and leaching along the soil profile.

5. Conclusions

We used a space-for-time substitution of soils under different land use scenarios to estimate continental-scale SOC change over 30 years across NEON domains, based on samples from 715 NEON soil profiles. We further

quantified environmental and edaphic effects on SOC change using structural equation models. This research not only demonstrates a framework to estimate SOC change using the currently available datasets, but also provides evaluation and feedback to the NEON team and other field scientists on additional sampling and archiving to ensure adequate estimation and/or monitoring of SOC change. Soil variability could be further controlled if more soil plots were sampled by reflecting the LCLUC or disturbance within the same soil order and the same domain.

We conclude that:

- The carbon sequestration potential of croplands and pastures requires careful assessment for credit-based carbon sequestration initiatives;
- Under the land-use change scenario of converting reference natural vegetation to disturbed natural vegetation, SOC did not change significantly. Ultisols, Spodosols, and Inceptisols showed a trend of SOC accumulation especially on the east coast, while Inceptisols, Andisols, and Aridisols in the western sites showed the trend of SOC loss;
- Compared with the same reference soils under natural vegetation, Mollisols and Alfisols showed a large SOC decrease due to farming and grazing in the central plains;
- Runoff/erosion and leaching potential, and mineral sorption were the dominant factors affecting SOC content across the NEON sites, and carbon cycle models may benefit from explicitly representing these processes.

Data Availability Statement

Data used to generate the SOC change are publicly available through NEON DP1.10047.001 (https://data.neonscience.org/data-products/DP1.10047.001). The Google Earth Engine code for land-use change detection is available through Google Earth Engine (https://code.earthengine.google.com/b92d66e33031ef0c115154cf0d6fd481). The R codes that support the SOC change calculation and SEM modeling of this study can be found at the repository: NEON_SOC_Change (https://zenodo.org/record/7850740). Sources and references of the environmental and soil datasets were given in Supporting Information S1 (Table S1). Mean SOC concentrations for each soil order and horizon under different land-cover subgroups within each eco-climatic domain were also provided in Data Set S1.

Acknowledgments

We acknowledge the National Ecological Observatory Network, United States Department of Agriculture Natural Resources Conservation Services (NRCS), the United States Department of Energy, Office of Science, Office of Biological and Environmental Research, and Kellogg Soil Survey Laboratory for conducting the research, collecting soil samples, and analyzing soil physical and chemical properties. Landsat-5, 7, and 8 image courtesy of the U.S. Geological Survey. We thank Dr. Steve Monteith from USDA NRCS Kellogg Soil Survey Laboratory for providing the Alaskan soil profiles archive. The Lawrence Berkeley National Laboratory (LBNL) is managed and operated by the University of California (UC) under U.S. Department of Energy Contract No. DE-AC02-05CH11231. Jingyi Huang and Alfred E. Hartemink were supported by NSF Signals in the Soil Grant 2226568. Jie Hu and Jingyi Huang were supported by the Champ Tanner Agricultural Physics Award and the University of Wisconsin–Madison Office of the Vice Chancellor for Research and Graduate Education with funding from the Wisconsin Alumni Research Foundation. Philip A. Townsend was supported by NSF Macrosystems Biology and NEON-Enabled Science Grant 1638720.

References

Abatzoglou, J. T., Dobrowski, S. Z., Parks, S. A., & Hegewisch, K. C. (2018). TerraClimate, a high-resolution global dataset of monthly climate and climatic water balance from 1958–2015. *Scientific Data*, *5*(1), 1–12. https://doi.org/10.1038/sdata.2017.191

Abramoff, R. Z., Guenet, B., Zhang, H., Georgiou, K., Xu, X., Viscarra Rossel, R. A., et al. (2022). Improved global-scale predictions of soil carbon stocks with Millennial Version 2. *Soil Biology and Biochemistry*, *164*, 108466. https://doi.org/10.1016/J.SOILBIO.2021.108466

Adhikari, K., Owens, P. R., Libohova, Z., Miller, D. M., Wills, S. A., & Nemecek, J. (2019). Assessing soil organic carbon stock of Wisconsin, USA and its fate under future land use and climate change. *Science of the Total Environment*, *667*, 833–845. https://doi.org/10.1016/j.scitotenv.2019.02.420

Ahrens, B., Braakhekke, M. C., Guggenberger, G., Schrumpf, M., & Reichstein, M. (2015). Contribution of sorption, DOC transport and microbial interactions to the 14C age of a soil organic carbon profile: Insights from a calibrated process model. *Soil Biology and Biochemistry*, *88*, 390–402. https://doi.org/10.1016/J.SOILBIO.2015.06.008

Ahrens, B., Guggenberger, G., Rethemeyer, J., John, S., Marschner, B., Heinze, S., et al. (2020). Combination of energy limitation and sorption capacity explains 14C depth gradients. *Soil Biology and Biochemistry*, *148*, 107912. https://doi.org/10.1016/J.SOILBIO.2020.107912

Amundson, R., & Biardeau, L. (2018). Opinion: Soil carbon sequestration is an elusive climate mitigation tool. *Proceedings of the National Academy of Sciences*, *115*(46), 11652–11656. https://doi.org/10.1073/PNAS.1815901115

Bloesch, P. M. (2012). Prediction of the CEC to clay ratio using mid-infrared spectroscopy. *Soil Research*, *50*(1), 1–6. https://doi.org/10.1071/SR11137

Blois, J. L., Williams, J. W., Fitzpatrick, M. C., Jackson, S. T., & Ferrier, S. (2013). Space can substitute for time in predicting climate-change effects on biodiversity. *Proceedings of the National Academy of Sciences of the United States of America*, *110*(23), 9374–9379. https://doi.org/10.1073/pnas.1220228110

Bonfatti, B. R., Hartemink, A. E., Giasson, E., Tornquist, C. G., & Adhikari, K. (2016). Digital mapping of soil carbon in a viticultural region of Southern Brazil. *Geoderma*, *261*, 204–221. https://doi.org/10.1016/j.geoderma.2015.07.016

Boysen, L. R., Brovkin, V., Warlind, D., Peano, D., Lanso, A. S., Delire, C., et al. (2021). Evaluation of soil carbon dynamics after forest cover change in CMIP6 land models using chronosequences. *Environmental Research Letters*, *16*(7), 074030. https://doi.org/10.1088/1748-9326/AC0BE1

Braakhekke, M. C., Beer, C., Hoosbeek, M. R., Reichstein, M., Kruijt, B., Schrumpf, M., & Kabat, P. (2011). SOMPROF: A vertically explicit soil organic matter model. *Ecological Modelling*, *222*(10), 1712–1730. https://doi.org/10.1016/J.ECOLMODEL.2011.02.015

Bruun, S., Christensen, B. T., Thomsen, I. K., Jensen, E. S., & Jensen, L. S. (2007). Modeling vertical movement of organic matter in a soil incubated for 41 years with 14C labeled straw. *Soil Biology and Biochemistry*, *39*(1), 368–371. https://doi.org/10.1016/J.SOILBIO.2006.07.003

Camino-Serrano, M., Guenet, B., Luyssaert, S., Ciais, P., Bastrikov, V., De Vos, B., et al. (2018). ORCHIDEE-SOM: Modeling soil organic carbon (SOC) and dissolved organic carbon (DOC) dynamics along vertical soil profiles in Europe. *Geoscientific Model Development*, *11*(3), 937–957. https://doi.org/10.5194/GMD-11-937-2018

Caspersen, J. P., Pacala, S. W., Jenkins, J. C., Hurtt, G. C., Moorcroft, P. R., & Birdsey, R. A. (2000). Contributions of land-use history to carbon accumulation in U.S. Forests. *Science*, *290*(5494), 1148–1151. https://doi.org/10.1126/SCIENCE.290.5494.1148

Conrad, O., Bechtel, B., Bock, M., Dietrich, H., Fischer, E., Gerlitz, L., et al. (2015). System for automated geoscientific analyses (SAGA) v. 2.1.4. *Geoscientific Model Development*, *8*(7), 1991–2007. https://doi.org/10.5194/GMD-8-1991-2015

Cotrufo, M. F., Wallenstein, M. D., Boot, C. M., Denef, K., & Paul, E. (2013). The microbial efficiency-matrix stabilization (MEMS) framework integrates plant litter decomposition with soil organic matter stabilization: Do labile plant inputs form stable soil organic matter? *Global Change Biology*, *19*(4), 988–995. https://doi.org/10.1111/GCB.12113

Driscoll, W. C. (1996). Robustness of the ANOVA and Tukey-Kramer statistical tests. *Computers & Industrial Engineering*, *31*(1–2), 265–268. https://doi.org/10.1016/0360-8352(96)00127-1

Eisenhauer, N., Bowker, M. A., Grace, J. B., & Powell, J. R. (2015). From patterns to causal understanding: Structural equation modeling (SEM) in soil ecology. *Pedobiologia*, *58*(2–3), 65–72. https://doi.org/10.1016/j.pedobi.2015.03.002

Eldridge, S. M. (2003). *A guide to characterising Australian sugarcane soils*. CRC. Retrieved from https://elibrary.sugarresearch.com.au/handle/11079/16449

Ellert, B. H., & Bettany, J. R. (2011). Calculation of organic matter and nutrients stored in soils under contrasting management regimes. *Canadian Journal of Soil Science*, *75*(4), 529–538. https://doi.org/10.4141/CJSS95-075

Erb, K. H., Luyssaert, S., Meyfroidt, P., Pongratz, J., Don, A., Kloster, S., et al. (2017). Land management: Data availability and process understanding for global change studies. *Global Change Biology*, *23*(2), 512–533. https://doi.org/10.1111/GCB.13443

Foga, S., Scaramuzza, P. L., Guo, S., Zhu, Z., Dilley, R. D., Beckmann, T., et al. (2017). Cloud detection algorithm comparison and validation for operational Landsat data products. *Remote Sensing of Environment*, *194*, 379–390. https://doi.org/10.1016/j.rse.2017.03.026

Friedl, M., & Sulla-Menashe, D. (2019). *MCD12Q1 MODIS/Terra+ aqua land cover type yearly L3 global 500m SIN grid V006*. NASA EOSDIS Land Processes DAAC: Sioux Falls. https://doi.org/10.5067/MODIS/MCD12Q1.006

Gautam, S., Mishra, U., Scown, C. D., Wills, S. A., Adhikari, K., Drewniak, B. A., & Waring, B. G. (2022). Continental United States may lose 1.8 petagrams of soil organic carbon under climate change by 2100. *Global Ecology and Biogeography*, *31*(6), 1147–1160. https://doi.org/10.1111/GEB.13489

Georgiou, K., Jackson, R. B., Vindušková, O., Abramoff, R. Z., Ahlström, A., Feng, W., et al. (2022). Global stocks and capacity of mineral-associated soil organic carbon. *Nature Communications*, *13*(1), 1–12. https://doi.org/10.1038/s41467-022-31540-9

Gifford, R. M., & Roderick, M. L. (2003). Soil carbon stocks and bulk density: Spatial or cumulative mass coordinates as a basis of expression? *Global Change Biology*, *9*(11), 1507–1514. https://doi.org/10.1046/J.1365-2486.2003.00677.X

Gonçalves, D. R. P., Mishra, U., Wills, S., & Gautam, S. (2021). Regional environmental controllers influence continental scale soil carbon stocks and future carbon dynamics. *Scientific Reports*, *11*(1), 1–10. https://doi.org/10.1038/s41598-021-85992-y

Gorelick, N., Hancher, M., Dixon, M., Ilyushchenko, S., Thau, D., & Moore, R. (2017). Google Earth Engine: Planetary-scale geospatial analysis for everyone. *Remote Sensing of Environment*, *202*, 18–27. https://doi.org/10.1016/j.rse.2017.06.031

Grace, J. B. (2006). *Structural equation modeling and natural systems*. Cambridge University Press.

Guber, A., Blagodatskaya, E., & Kravchenko, A. (2022). Are enzymes transported in soils by water fluxes? *Soil Biology and Biochemistry*, *168*, 108633. https://doi.org/10.1016/J.SOILBIO.2022.108633

Guillaume, T., Bragazza, L., Levasseur, C., Libohova, Z., & Sinaj, S. (2021). Long-term soil organic carbon dynamics in temperate cropland-grassland systems. *Agriculture, Ecosystems & Environment*, *305*, 107184. https://doi.org/10.1016/j.agee.2020.107184

Guillaume, T., Makowski, D., Libohova, Z., Bragazza, L., Sallaku, F., & Sinaj, S. (2022). Soil organic carbon saturation in cropland-grassland systems: Storage potential and soil quality. *Geoderma*, *406*, 115529. https://doi.org/10.1016/j.geoderma.2021.115529

Gurney, K., & Shepson, P. (2021). Opinion: The power and promise of improved climate data infrastructure. *Proceedings of the National Academy of Sciences of the United States of America*, *118*(35). https://doi.org/10.1073/PNAS.2114115118

Hargrove, W. W., & Hoffman, F. M. (2004). Potential of multivariate quantitative methods for delineation and visualization of ecoregions. *Environmental Management*, *34*(5), S39–S60. https://doi.org/10.1007/S00267-003-1084-0

Huang, J., & Hartemink, A. E. (2020). Soil and environmental issues in sandy soils. *Earth-Science Reviews*, *208*, 103295. https://doi.org/10.1016/j.earscirev.2020.103295

Humphrey, V., Berg, A., Ciais, P., Gentine, P., Jung, M., Reichstein, M., et al. (2021). Soil moisture–atmosphere feedback dominates land carbon uptake variability. *Nature*, *592*(7852), 65–69. https://doi.org/10.1038/s41586-021-03325-5

Jenny, H. (1994). *Factors of soil formation: A system of quantitative pedology*. Courier Corporation.

Jobbágy, E. G., & Jackson, R. B. (2000). The vertical distribution of soil organic carbon and its relation to climate and vegetation. *Ecological Applications*, *10*(2), 423–436. https://doi.org/10.1890/1051-0761(2000)010[0423:TVDOSO]2.0.CO;2

Kaiser, M., Kleber, M., & Berhe, A. A. (2015). How air-drying and rewetting modify soil organic matter characteristics: An assessment to improve data interpretation and inference. *Soil Biology and Biochemistry*, *80*, 324–340. https://doi.org/10.1016/J.SOILBIO.2014.10.018

Kravchenko, A. N., Guber, A. K., Razavi, B. S., Koestel, J., Quigley, M. Y., Robertson, G. P., & Kuzyakov, Y. (2019). Microbial spatial footprint as a driver of soil carbon stabilization. *Nature Communications*, *10*(1), 1–10. https://doi.org/10.1038/s41467-019-11057-4

Lal, R. (1999). Soil management and restoration for C sequestration to mitigate the accelerated greenhouse effect. *Progress in Environmental Science*, *1*(4), 307–326.

Lal, R. (2003). Soil erosion and the global carbon budget. *Environment International*, *29*(4), 437–450. https://doi.org/10.1016/S0160-4120(02)00192-7

Lal, R. (2004). Soil carbon sequestration to mitigate climate change. *Geoderma*, *123*(1–2), 1–22. https://doi.org/10.1016/j.geoderma.2004.01.032

Lasslop, G., Brovkin, V., Reick, C. H., Bathiany, S., & Kloster, S. (2016). Multiple stable states of tree cover in a global land surface model due to a fire-vegetation feedback. *Geophysical Research Letters*, *43*(12), 6324–6331. https://doi.org/10.1002/2016GL069365

Li, H., Wu, Y., Liu, S., Xiao, J., Zhao, W., Chen, J., et al. (2022). Decipher soil organic carbon dynamics and driving forces across China using machine learning. *Global Change Biology*, *00*(10), 1–17. https://doi.org/10.1111/GCB.16154

Lugato, E., Leip, A., & Jones, A. (2018). Mitigation potential of soil carbon management overestimated by neglecting N_2O emissions. *Nature Climate Change*, *8*(3), 219–223. https://doi.org/10.1038/s41558-018-0087-z

Luo, Z., Viscarra-Rossel, R. A., & Qian, T. (2021). Similar importance of edaphic and climatic factors for controlling soil organic carbon stocks of the world. *Biogeosciences*, *18*(6), 2063–2073. https://doi.org/10.5194/bg-18-2063-2021

Luo, Z., Wang, G., & Wang, E. (2019). Global subsoil organic carbon turnover times dominantly controlled by soil properties rather than climate. *Nature Communications*, *10*(1), 3688. https://doi.org/10.1038/s41467-019-11597-9

McPartland, M. Y., Kane, E. S., Falkowski, M. J., Kolka, R., Turetsky, M. R., Palik, B., & Montgomery, R. A. (2019). The response of boreal peatland community composition and NDVI to hydrologic change, warming, and elevated carbon dioxide. *Global Change Biology*, *25*(1), 93–107. https://doi.org/10.1111/GCB.14465

Moreland, K., Tian, Z., Berhe, A. A., McFarlane, K. J., Hartsough, P., Hart, S. C., et al. (2021). Deep in the Sierra Nevada critical zone: Saprock represents a large terrestrial organic carbon stock. *Environmental Research Letters*, *16*(12), 124059. https://doi.org/10.1088/1748-9326/AC3BFE

Nahlik, A. M., & Fennessy, M. S. (2016). Carbon storage in US wetlands. *Nature Communications*, *7*(1), 1–9. https://doi.org/10.1038/ncomms13835

Nakhavali, M., Lauerwald, R., Regnier, P., Guenet, B., Chadburn, S., & Friedlingstein, P. (2021). Leaching of dissolved organic carbon from mineral soils plays a significant role in the terrestrial carbon balance. *Global Change Biology*, *27*(5), 1083–1096. https://doi.org/10.1111/GCB.15460

Nave, L. E., Bowman, M., Gallo, A., Hatten, J. A., Heckman, K. A., Matosziuk, L., et al. (2021). Patterns and predictors of soil organic carbon storage across a continental-scale network. *Biogeochemistry*, *156*(1), 75–96. https://doi.org/10.1007/S10533-020-00745-9/TABLES/7

Nave, L. E., Domke, G. M., Hofmeister, K. L., Mishra, U., Perry, C. H., Walters, B. F., & Swanston, C. W. (2018). Reforestation can sequester two petagrams of carbon in US topsoils in a century. *Proceedings of the National Academy of Sciences of the United States of America*, *115*(11), 2776–2781. https://doi.org/10.1073/PNAS.1719685115/SUPPL_FILE/PNAS.201719685SI

NEON. (2020). *Soil physical and chemical properties, periodic (DP1.10047.001)*. National Ecological Observatory Network (NEON). https://doi.org/10.48443/X9AJ-3647

Page, S. E., Rieley, J. O., & Banks, C. J. (2011). Global and regional importance of the tropical peatland carbon pool. *Global Change Biology*, *17*(2), 798–818. https://doi.org/10.1111/J.1365-2486.2010.02279.X

Pearring, J. R. (1968). *A study of basic mineralogical, physical-chemical, and engineering index properties of laterite soils*. Texas A&M University.

Pickett, S. T. A. (1989). Space-for-Time substitution as an alternative to long-term studies. In *Long-term studies in ecology* (pp. 110–135). Springer. https://doi.org/10.1007/978-1-4615-7358-6_5

Post, W. M., & Kwon, K. C. (2000). Soil carbon sequestration and land-use change: Processes and potential. *Global Change Biology*, *6*(3), 317–327. https://doi.org/10.1046/j.1365-2486.2000.00308.x

Quan, Q., Tian, D., Luo, Y., Zhang, F., Crowther, T. W., Zhu, K., et al. (2019). Water scaling of ecosystem carbon cycle feedback to climate warming. *Science Advances*, *5*(8). https://doi.org/10.1126/SCIADV.AAV1131/SUPPL_FILE/AAV1131_SM.PDF

Rasmussen, C., Heckman, K., Wieder, W. R., Keiluweit, M., Lawrence, C. R., Berhe, A. A., et al. (2018). Beyond clay: Towards an improved set of variables for predicting soil organic matter content. *Biogeochemistry*, *137*(3), 297–306. https://doi.org/10.1007/S10533-018-0424-3/FIGURES/3

Rosseel, Y. (2012). lavaan: An R package for structural equation modeling. *Journal of Statistical Software*, *48*(2), 1–36. https://doi.org/10.18637/JSS.V048.I02

Rui, Y., Jackson, R. D., Cotrufo, M. F., Sanford, G. R., Spiesman, B. J., Deiss, L., et al. (2022). Persistent soil carbon enhanced in Mollisols by well-managed grasslands but not annual grain or dairy forage cropping systems. *Proceedings of the National Academy of Sciences*, *119*(7), e2118931119. https://doi.org/10.1073/PNAS.2118931119

Sanford, G. R., Posner, J. L., Jackson, R. D., Kucharik, C. J., Hedtcke, J. L., & Lin, T. L. (2012). Soil carbon lost from Mollisols of the North Central U.S.A. with 20 years of agricultural best management practices. *Agriculture, Ecosystems & Environment*, *162*, 68–76. https://doi.org/10.1016/j.agee.2012.08.011

Scharlemann, J. P. W., Tanner, E. V. J., Hiederer, R., & Kapos, V. (2014). *Global soil carbon: Understanding and managing the largest terrestrial carbon pool*. Carbon Management. Future Science LtdLondon. https://doi.org/10.4155/cmt.13.77

Schimel, D., Hargrove, W., Hoffman, F., & MacMahon, J. (2007). NEON: A hierarchically designed national ecological network. *Frontiers in Ecology and the Environment*, *5*(2), 59. https://doi.org/10.1890/1540-9295(2007)5[59:nahdne]2.0.co;2

Schlesinger, W. H., & Amundson, R. (2019). Managing for soil carbon sequestration: Let's get realistic. *Global Change Biology*, *25*(2), 386–389. https://doi.org/10.1111/GCB.14478

Schmidt, G., Jenkerson, C., Masek, J., Vermote, E., & Gao, F. (2013). Landsat ecosystem disturbance adaptive processing system (LEDAPS) algorithm description Open-File Report. Retrieved from http://www.usgs.gov/pubprod

Shen, Y. H. (1999). Sorption of natural dissolved organic matter on soil. *Chemosphere*, *38*(7), 1505–1515. https://doi.org/10.1016/S0045-6535(98)00371-3

Six, J., Conant, R. T., Paul, E. A., & Paustian, K. (2002). Stabilization mechanisms of soil organic matter: Implications for C-saturation of soils. *Plant and Soil*, *241*(2), 155–176. https://doi.org/10.1023/A:1016125726789

Smith, B., Prentice, I. C., & Sykes, M. T. (2001). Representation of vegetation dynamics in the modelling of terrestrial ecosystems: Comparing two contrasting approaches within European climate space. *Global Ecology and Biogeography*, *10*(6), 621–637. https://doi.org/10.1046/J.1466-822X.2001.T01-1-00256.X

Smith, P., House, J. I., Bustamante, M., Sobocká, J., Harper, R., Pan, G., et al. (2016). Global change pressures on soils from land use and management. *Global Change Biology*, *22*(3), 1008–1028. https://doi.org/10.1111/GCB.13068

Snyder, C. S., Bruulsema, T. W., Jensen, T. L., & Fixen, P. E. (2009). Review of greenhouse gas emissions from crop production systems and fertilizer management effects. *Agriculture, Ecosystems & Environment*, *133*(3–4), 247–266. https://doi.org/10.1016/J.AGEE.2009.04.021

Soil Survey Staff. (2014). In R. Burt & Soil Survey Staff (Eds.), *Kellog soil survey laboratory methods manual. Soil survey investigations report No. 42, version 5.0*. U.S. Department of Agriculture, Natural Resources Conservation Service.

Solly, E. F., Weber, V., Zimmermann, S., Walthert, L., Hagedorn, F., & Schmidt, M. W. I. (2020). A critical evaluation of the relationship between the effective cation exchange capacity and soil organic carbon content in Swiss forest soils. *Frontiers in Forests and Global Change*, *3*, 98. https://doi.org/10.3389/ffgc.2020.00098

Stewart, C. E., Paustian, K., Conant, R. T., Plante, A. F., & Six, J. (2007). Soil carbon saturation: Concept, evidence and evaluation. *Biogeochemistry*, *86*(1), 19–31. https://doi.org/10.1007/S10533-007-9140-0/FIGURES/5

Sulman, B. N., Moore, J. A. M., Abramoff, R., Averill, C., Kivlin, S., Georgiou, K., et al. (2018). Multiple models and experiments underscore large uncertainty in soil carbon dynamics. *Biogeochemistry*, *141*(2), 109–123. https://doi.org/10.1007/S10533-018-0509-Z

Sulman, B. N., Phillips, R. P., Oishi, A. C., Shevliakova, E., & Pacala, S. W. (2014). Microbe-driven turnover offsets mineral-mediated storage of soil carbon under elevated CO_2. *Nature Climate Change*, *4*(12), 1099–1102. https://doi.org/10.1038/nclimate2436

Sun, W., Canadell, J. G., Yu, L., Yu, L., Zhang, W., Smith, P., et al. (2020). Climate drives global soil carbon sequestration and crop yield changes under conservation agriculture. *Global Change Biology*, *26*(6), 3325–3335. https://doi.org/10.1111/GCB.15001

Tan, Z., & Lal, R. (2005). Carbon sequestration potential estimates with changes in land use and tillage practice in Ohio, USA. *Agriculture, Ecosystems & Environment*, *111*(1–4), 140–152. https://doi.org/10.1016/J.AGEE.2005.05.012

Tan, Z., Lal, R., Smeck, N. E., Calhoun, F. G., Slater, B. K., Parkinson, B., & Gehring, R. M. (2004). Taxonomic and geographic distribution of soil organic carbon pools in Ohio. *Soil Science Society of America Journal*, *68*(6), 1896–1904. https://doi.org/10.2136/SSSAJ2004.1896

Tang, X., Zhao, X., Bai, Y., Tang, Z., Wang, W., Zhao, Y., et al. (2018). Carbon pools in China's terrestrial ecosystems: New estimates based on an intensive field survey. *Proceedings of the National Academy of Sciences of the United States of America*, *115*(16), 4021–4026. https://doi.org/10.1073/pnas.1700291115

Tarnocai, C., Canadell, J. G., Schuur, E. A. G., Kuhry, P., Mazhitova, G., & Zimov, S. (2009). Soil organic carbon pools in the northern circumpolar permafrost region. *Global Biogeochemical Cycles*, *23*(2), GB2023. https://doi.org/10.1029/2008GB003327

Tifafi, M., Guenet, B., & Hatté, C. (2018). Large differences in global and regional total soil carbon stock estimates based on SoilGrids, HWSD, and NCSCD: Intercomparison and evaluation based on field data from USA, England, Wales, and France. *Global Biogeochemical Cycles*, *32*(1), 42–56. https://doi.org/10.1002/2017GB005678

Tong, X., Brandt, M., Yue, Y., Ciais, P., Rudbeck Jepsen, M., Penuelas, J., et al. (2020). Forest management in southern China generates short term extensive carbon sequestration. *Nature Communications*, *11*(1), 1–10. https://doi.org/10.1038/s41467-019-13798-8

Torn, M. S., Trumbore, S. E., Chadwick, O. A., Vitousek, P. M., & Hendricks, D. M. (1997). Mineral control of soil organic carbon storage and turnover. *Nature*, *389*(6647), 170–173. https://doi.org/10.1038/38260

Tugel, A. J., Herrick, J. E., Brown, J. R., Mausbach, M. J., Puckett, W., & Hipple, K. (2005). Soil change, soil survey, and natural resources decision making. *Soil Science Society of America Journal*, *69*(3), 738–747. https://doi.org/10.2136/sssaj2004.0163

U.S. Geological Survey. (2020). *1/3rd arc-second digital elevation models (DEMs) - USGS national map 3DEP downloadable data collection*. U.S. Geological Survey.

Vermote, E., Roger, J. C., Franch, B., & Skakun, S. (2018). LASRC (land surface reflectance code): Overview, application and validation using MODIS, VIIRS, LANDSAT and Sentinel 2 data's. In *International geoscience and remote sensing symposium (IGARSS)* (Vol. 2018-July, pp. 8173–8176). Institute of Electrical and Electronics Engineers Inc. https://doi.org/10.1109/IGARSS.2018.8517622

Wang, G., Post, W. M., & Mayes, M. A. (2013). Development of microbial-enzyme-mediated decomposition model parameters through steady-state and dynamic analyses. *Ecological Applications*, *23*(1), 255–272. https://doi.org/10.1890/12-0681.1

Waring, C., Stockmann, U., Malone, B. P., Whelan, B., & McBratney, A. B. (2014). Is percent 'projected natural vegetation soil carbon' a useful indicator of soil condition? In *Soil carbon* (pp. 219–227). Springer International Publishing. https://doi.org/10.1007/978-3-319-04084-4_23

Wattel-Koekkoek, E. J. W., Van Genuchten, P. P. L., Buurman, P., & Van Lagen, B. (2001). Amount and composition of clay-associated soil organic matter in a range of kaolinitic and smectitic soils. *Geoderma*, *99*(1–2), 27–49. https://doi.org/10.1016/S0016-7061(00)00062-8

Wendt, J. W., & Hauser, S. (2013). An equivalent soil mass procedure for monitoring soil organic carbon in multiple soil layers. *European Journal of Soil Science*, *64*(1), 58–65. https://doi.org/10.1111/EJSS.12002

Wieder, W. R., Allison, S. D., Davidson, E. A., Georgiou, K., Hararuk, O., He, Y., et al. (2015). Explicitly representing soil microbial processes in Earth system models. *Global Biogeochemical Cycles*, *29*(10), 1782–1800. https://doi.org/10.1002/2015GB005188

Wieder, W. R., Grandy, A. S., Kallenbach, C. M., & Bonan, G. B. (2014). Integrating microbial physiology and physio-chemical principles in soils with the MIcrobial-MIneral Carbon Stabilization (MIMICS) model. *Biogeosciences*, *11*(14), 3899–3917. https://doi.org/10.5194/BG-11-3899-2014

Wiesmeier, M., Hübner, R., Spörlein, P., Geuß, U., Hangen, E., Reischl, A., et al. (2014). Carbon sequestration potential of soils in southeast Germany derived from stable soil organic carbon saturation. *Global Change Biology*, *20*(2), 653–665. https://doi.org/10.1111/GCB.12384

Wiesmeier, M., Spörlein, P., Geuß, U., Hangen, E., Haug, S., Reischl, A., et al. (2012). Soil organic carbon stocks in southeast Germany (Bavaria) as affected by land use, soil type and sampling depth. *Global Change Biology*, *18*(7), 2233–2245. https://doi.org/10.1111/J.1365-2486.2012.02699.X

Wiesmeier, M., von Lützow, M., Spörlein, P., Geuß, U., Hangen, E., Reischl, A., et al. (2015). Land use effects on organic carbon storage in soils of Bavaria: The importance of soil types. *Soil and Tillage Research*, *146*(PB), 296–302. https://doi.org/10.1016/J.STILL.2014.10.003

Wilson, R. M., Hopple, A. M., Tfaily, M. M., Sebestyen, S. D., Schadt, C. W., Pfeifer-Meister, L., et al. (2016). Stability of peatland carbon to rising temperatures. *Nature Communications*, *7*(1), 1–10. https://doi.org/10.1038/ncomms13723

Wulder, M. A., White, J. C., Loveland, T. R., Woodcock, C. E., Belward, A. S., Cohen, W. B., et al. (2016). The global Landsat archive: Status, consolidation, and direction. *Remote Sensing of Environment*, *185*, 271–283. https://doi.org/10.1016/J.RSE.2015.11.032

Yang, Y., Tilman, D., Furey, G., & Lehman, C. (2019). Soil carbon sequestration accelerated by restoration of grassland biodiversity. *Nature Communications*, *10*(1), 1–7. https://doi.org/10.1038/s41467-019-08636-w

Yu, L., Ahrens, B., Wutzler, T., Schrumpf, M., & Zaehle, S. (2020). Jena soil model (JSM v1.0; Revision 1934): A microbial soil organic carbon model integrated with nitrogen and phosphorus processes. *Geoscientific Model Development*, *13*(2), 783–803. https://doi.org/10.5194/GMD-13-783-2020

Zhang, Q., Hou, C., Liang, Y., & Feng, Y. (2014). Dissolved organic matter release and retention in Ultisols in relation to land use patterns. *Chemosphere*, *107*, 432–438. https://doi.org/10.1016/J.CHEMOSPHERE.2014.01.043

Zhang, Q., Shao, M., Jia, X., & Wei, X. (2019). Changes in soil physical and chemical properties after short drought stress in semi-humid forests. *Geoderma*, *338*, 170–177. https://doi.org/10.1016/J.GEODERMA.2018.11.051

Zhu, Z., & Woodcock, C. E. (2012). Object-based cloud and cloud shadow detection in Landsat imagery. *Remote Sensing of Environment*, *118*, 83–94. https://doi.org/10.1016/J.RSE.2011.10.028

Zhu, Z., & Woodcock, C. E. (2014). Continuous change detection and classification of land cover using all available Landsat data. *Remote Sensing of Environment*, *144*, 152–171. https://doi.org/10.1016/j.rse.2014.01.011

Zhu, Z., Woodcock, C. E., Holden, C., & Yang, Z. (2015). Generating synthetic Landsat images based on all available Landsat data: Predicting Landsat surface reflectance at any given time. *Remote Sensing of Environment*, *162*, 67–83. https://doi.org/10.1016/J.RSE.2015.02.009

Zhu, Z., Zhang, J., Yang, Z., Aljaddani, A. H., Cohen, W. B., Qiu, S., & Zhou, C. (2020). Continuous monitoring of land disturbance based on Landsat time series. *Remote Sensing of Environment*, *238*, 111116. https://doi.org/10.1016/J.RSE.2019.03.009

References From the Supporting Information

Berner, L. T., Massey, R., Jantz, P., Forbes, B. C., Macias-Fauria, M., Myers-Smith, I., et al. (2020). Summer warming explains widespread but not uniform greening in the Arctic tundra biome. *Nature Communications*, *11*(1), 1–12. https://doi.org/10.1038/s41467-020-18479-5

Bockheim, J. G., & Tarnocai, C. (1998). Recognition of cryoturbation for classifying permafrost-affected soils. *Geoderma*, *81*(3–4), 281–293. https://doi.org/10.1016/S0016-7061(97)00115-8

Chang, R., Liu, S., Chen, L., Li, N., Bing, H., Wang, T., et al. (2021). Soil organic carbon becomes newer under warming at a permafrost site on the Tibetan Plateau. *Soil Biology and Biochemistry*, *152*, 108074. https://doi.org/10.1016/j.soilbio.2020.108074

Goetz, S. J., Bunn, A. G., Fiske, G. J., & Houghton, R. A. (2005). Satellite-observed photosynthetic trends across boreal North America associated with climate and fire disturbance. *Proceedings of the National Academy of Sciences*, *102*(38), 13521–13525. https://doi.org/10.1073/PNAS.0506179102

Grosse, G., Harden, J., Turetsky, M., McGuire, A. D., Camill, P., Tarnocai, C., et al. (2011). Vulnerability of high-latitude soil organic carbon in North America to disturbance. *Journal of Geophysical Research*, *116*, G00K06. https://doi.org/10.1029/2010JG001507

Harden, J. W., Meier, R., Silapaswan, C., Swanson, D. K., & McGuire, A. D. (2003). Soil drainage and its potential for influencing. *Studies by the US Geological Survey in Alaska*, *1678*, 139.

Jaffé, R., Ding, Y., Niggemann, J., Vähätalo, A. V., Stubbins, A., Spencer, R. G. M., et al. (2013). Global charcoal mobilization from soils via dissolution and riverine transport to the oceans. *Science*, *340*(6130), 345–347. https://doi.org/10.1126/science.1231476

Koven, C. D., Ringeval, B., Friedlingstein, P., Ciais, P., Cadule, P., Khvorostyanov, D., et al. (2011). Permafrost carbon-climate feedbacks accelerate global warming. *Proceedings of the National Academy of Sciences of the United States of America*, *108*(36), 14769–14774. https://doi.org/10.1073/pnas.1103910108

Mekonnen, Z. A., Riley, W. J., & Grant, R. F. (2018). 21st century tundra shrubification could enhance net carbon uptake of North America Arctic tundra under an RCP8.5 climate trajectory. *Environmental Research Letters*, *13*(5), 054029. https://doi.org/10.1088/1748-9326/AABF28

Myneni, R. B., Keeling, C. D., Tucker, C. J., Asrar, G., & Nemani, R. R. (1997). Increased plant growth in the northern high latitudes from 1981 to 1991. *Nature*, *386*(6626), 698–702. https://doi.org/10.1038/386698a0

Natali, S. M., Watts, J. D., Rogers, B. M., Potter, S., Ludwig, S. M., Selbmann, A.-K., et al. (2019). Large loss of CO_2 in winter observed across the northern permafrost region. *Nature Climate Change*, *9*(11), 852–857. https://doi.org/10.1038/s41558-019-0592-8

Ohlson, M., Dahlberg, B., Økland, T., Brown, K. J., & Halvorsen, R. (2009). The charcoal carbon pool in boreal forest soils. *Nature Geoscience*, *2*(10), 692–695. https://doi.org/10.1038/ngeo617

Ping, C. L., Bockheim, J. G., Kimble, J. M., Michaelson, G. J., & Walker, D. A. (1998). Characteristics of cryogenic soils along a latitudinal transect in Arctic Alaska. *Journal of Geophysical Research*, *103*(D22), 28917–28928. https://doi.org/10.1029/98JD02024

Rieger, S., Schoephorster, D. B., & Furbush, C. E. (1979). *Exploratory soil survey of Alaska*. US Department of Agriculture, Soil Conservation Service.

Riordan, B., Verbyla, D., & McGuire, A. D. (2006). Shrinking ponds in subarctic Alaska based on 1950–2002 remotely sensed images. *Journal of Geophysical Research*, *111*(G4), 4002. https://doi.org/10.1029/2005JG000150

Robinson, N. P., Allred, B. W., Smith, W. K., Jones, M. O., Moreno, A., Erickson, T. A., et al. (2018). Terrestrial primary production for the conterminous United States derived from Landsat 30 m and MODIS 250 m. *Remote Sensing in Ecology and Conservation*, *4*(3), 264–280. https://doi.org/10.1002/RSE2.74

Running, S., & Zhao, M. (2019). MOD17A3HGF MODIS/Terra Net Primary Production Gap-Filled Yearly L4 Global 500 m SIN Grid V006 [Dataset]. NASA EOSDIS Land Processes DAAC. https://doi.org/10.5067/MODIS/MOD17A3HGF.006

Schuur, E. A. G., McGuire, A. D., Schädel, C., Grosse, G., Harden, J. W., Hayes, D. J., et al. (2015). Climate change and the permafrost carbon feedback. *Nature*, *520*(7546), 171–179. https://doi.org/10.1038/nature14338

Sistla, S. A., Moore, J. C., Simpson, R. T., Gough, L., Shaver, G. R., & Schimel, J. P. (2013). Long-term warming restructures Arctic tundra without changing net soil carbon storage. *Nature*, *497*(7451), 615–617. https://doi.org/10.1038/nature12129

Treseder, K. K., Mack, M. C., & Cross, A. (2004). Relationships among fires, fungi, and soil dynamics in Alaskan boreal forests. *Ecological Applications*, *14*(6), 1826–1838. https://doi.org/10.1890/03-5133

Verbyla, D. (2008). The greening and browning of Alaska based on 1982–2003 satellite data. *Global Ecology and Biogeography*, *17*(4), 547–555. https://doi.org/10.1111/J.1466-8238.2008.00396.X

Waldrop, M. P., & Harden, J. W. (2008). Interactive effects of wildfire and permafrost on microbial communities and soil processes in an Alaskan black spruce forest. *Global Change Biology*, *14*(11), 2591–2602. https://doi.org/10.1111/j.1365-2486.2008.01661.x

Yoshikawa, K., & Hinzman, L. D. (2003). Shrinking thermokarst ponds and groundwater dynamics in discontinuous permafrost near council, Alaska. *Permafrost and Periglacial Processes*, *14*(2), 151–160. https://doi.org/10.1002/PPP.451

Zhu, Z., Piao, S., Myneni, R. B., Huang, M., Zeng, Z., Canadell, J. G., et al. (2016). Greening of the Earth and its drivers. *Nature Climate Change*, *6*(8), 791–795. https://doi.org/10.1038/nclimate3004